FOREWORD

This report was prepared by the Research Laboratories of Westinghouse Electric Corporation under USAF Contract No. AF 33(616)-7888. The contract was initiated under Project No. 7351, "Metallic Materials," Task No. 735101, "Refractory Materials." The work was administered under the direction of the Directorate of Materials and Processes, Deputy Commander/ Technology, Aeronautical Systems Division, Wright-Patterson Air Force Base, Ohio. Lt. W. E. Smith of the High Temperature Metals Section of the Physical Metallurgy Branch of the Directorate of Materials and Processes, was the project engineer in the early part of this contract. The latter part was monitored by Mr. P. L. Faust of the Electrochemical Section.

This report covers work conducted from January 1961 to January 1962.

The authors are indebted to M. J. Pantlik for his assistance in modification of our electron diffraction apparatus, in the construction of the Kanthal-Super furnace and in the construction of the oxygen consumption apparatus.

4-76C, 300, 9-24-62

ABSTRACT

This paper describes new experimental work on the oxidation of tungsten and a 50 weight percent tantalum-tungsten alloy.

The kinetics of oxidation were measured in a special ceramic tube reaction system using both weight change and oxygen consumption measurements. Above 1250°C tungsten trioxide volatilized as fast as it was formed in the reaction. Difficulties were found in using alumina furnace tubes in the presence of tungsten trioxide vapor which limited the maximum temperatures to 1615°C. Alumina tubes were found to crack on exposure to tungsten trioxide vapors for 10 to 15 minutes at 1615°C.

The rates of oxidation of tungsten were determined from 1150° to 1615°C in oxygen pressures of 2 to 100 Torr. Very high rates of oxidation or surface recession rates were found above 1200°C. An exponential temperature behavior for the rate of oxidation was found for all of the pressures studied. A heat of activation of 14,300 calories per mole was estimated from the data. A study of the effect of pressure on the rate of oxidation showed the following empirical equation could explain the weight loss data, $\frac{dw}{dt} = KP^{1.122}$. A theoretical analysis of the data using the absolute reaction rate theory suggested that the rate of oxidation of tungsten was limited by a mobile adsorption process of oxygen onto a tungsten surface already covered by a surface layer of oxide.

Oxidation of a 50 w/o tantalum-tungsten alloy was studied over the temperature range of 1068° to 1458°C at 152 Torr oxygen pressure. The results showed that a protective scale was formed on this alloy. The oxidation resistance was improved to a considerable extent over that of either of the pure metals or of other tungsten-tantalum alloys. There was some evidence that the scale formed on this alloy was $Ta_{10}W_8O_{49}$.

A special 250 kv electron diffraction camera was developed for the study of the tungsten-gas reacting interface. Preliminary diffraction data have been obtained on the oxidation of tungsten at temperatures of 800 to 1000°C.

This report has been reviewed and is approved.

I. PERLMUTTER
Chief, Physical Metallurgy Branch
Metals and Ceramics Laboratory
Directorate of Materials & Processes

TABLE OF CONTENTS

LIST OF ILLUSTRATIONS

LIST OF TABLES

OXIDATION OF TUNGSTEN AND TUNGSTEN BASED ALLOYS

GENERAL INTRODUCTION

This report covers the results obtained during the past year on studies of the oxidation of tungsten and tungsten based alloys. The background for this study was described in two previous reports, WADC Technical Report 59-575 Parts I and II. These reports included studies on the thermodynamics and kinetics of the oxidation process and structural determinations of the oxidation product.

The thermodynamic studies included the following: (1) Vapor pressure measurements over the tungsten oxides and mixed oxides of tungsten with hafnium and tantalum; (2) Calculations of the thermal properties of $W_{18}O_{19}$ and $W_{20}O_{58}$; and (3) Phase diagram studies.

The kinetics phase of the program consisted of determining oxidation rates as a function of temperature and pressure on the following: (1) pure tungsten sheet specimens from 500°-1300°C at oxygen pressures of 10^{-1}-10^{-3} atmospheres; (2) tungsten-tantalum alloys to 1200°C; and (3) inductively heated tungsten specimens from 800°-1698°C. The effect of oxygen pressure and the vaporization of WO_3 on the oxidation of cylindrical shaped specimens from 950°-1200°C was also determined. Selected specimens of the reaction products of the above oxidation studies were analyzed by x-ray diffraction and metallographic techniques.

During the past year we have continued the kinetic studies, developed and improved our apparatus and techniques and made a theoretical analysis of our results. The kinetic studies were made from 1150°C-1615°C and from 2-100 Torr of oxygen on cylindrical tungsten specimens. A 50 w/o tungsten-tantalum alloy was studied from 1068°C-1458°C at 0.2 atmosphere of oxygen.

Our apparatus and technique developments included an oxygen consumption method for the study of rapid oxidation reactions, a Kanthal-Super furnace for temperatures to 1665°C and a 250 KV electron diffraction camera for the study of gas metal interfaces during oxidation.

Manuscript released by authors December 1961 for publication as an ASD Technical Report.

SECTION I. KINETICS OF OXIDATION OF PURE TUNGSTEN, 1150°C-1615°C

INTRODUCTION

A number of studies have been made on the oxidation of tungsten below 1200°C. The literature and the results of these studies were discussed in WADC Technical Reports 59-575 Parts I and II.

Langmuir[1] was the first to study the reaction of tungsten with oxygen at temperatures above 1200°C. In this classic work tungsten filaments were heated electrically in oxygen at low pressures and the reaction followed by observation of the pressure. Filament temperatures between 1070° and 2770°K were used. Langmuir's results showed a continuous increase in reaction rate up to the highest temperature. The rate of reaction was found to be a linear function of pressure below a pressure of 10^{-3} Torr. No suggestion was reported concerning a change in rate of reaction above 2200°K.

Perkins and Crooks[2] used a modified Langmuir method. Direct electrical heating was used with the rate being determined by direct measure of the surface recession. One of the interesting features of this work was the finding of a decrease in rate of surface recession above 1900°C. Perkins and Crooks relate this inversion in the rate of surface recession to thermal dissociation of tungsten trioxide.

Our study is directed toward an understanding of the mechanism of oxidation of tungsten from 1150° to 1615°C over a wide pressure range. Unfortunately, our methods were not possible to use above 1615°C.

EXPERIMENTAL

Kinetic studies on the oxidation of pure tungsten were made using a sensitive weight change method and an oxygen consumption method. Both measuring systems were described in WADC Technical Report 59-575, Part II. The device for studying the oxygen consumed by tungsten during oxidation was made more operable by the addition of an improved type variable leak valve to the system.

1. Microbalance

Since large weight changes were involved during oxidation the gold plated Invar beam balance shown in Figure 1 was used. The balance had a beam length of 14.5 cm and a beam weight of 46 grams. Calibration of the balance showed a sensitivity of 60 micrograms for a 0.001 cm deflection at 7.25 cm using a weight of 0.83 g. The specimens were suspended using a 2 mil nickel-chromium alloy wire in the cold zone and an 8 mil section of platinum wire in the hot zone of the furnace tube.

2. Pressure Measuring System

A schematic diagram of the apparatus is shown in Figure 2 while a photograph

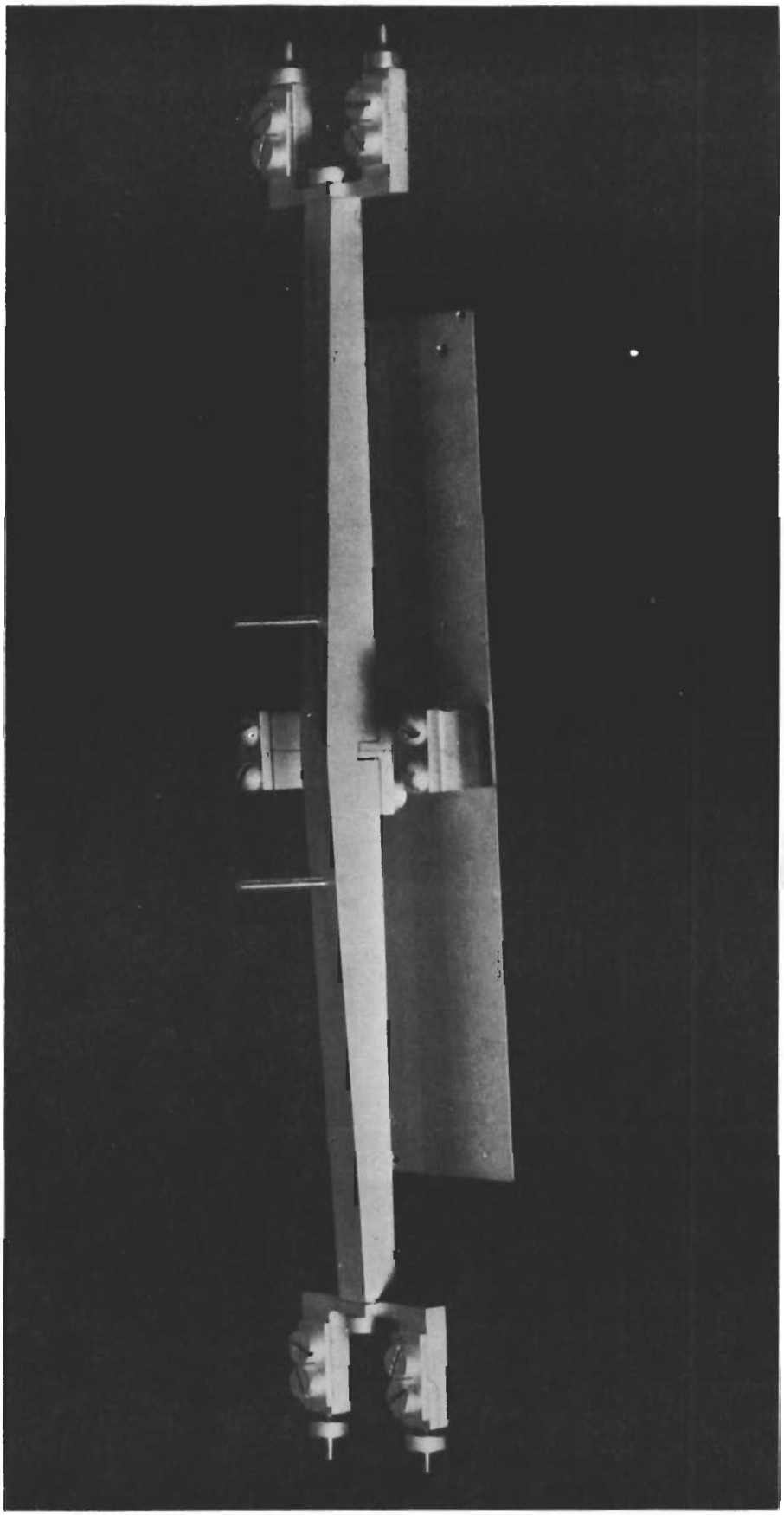

Fig. 1— Invar Balance

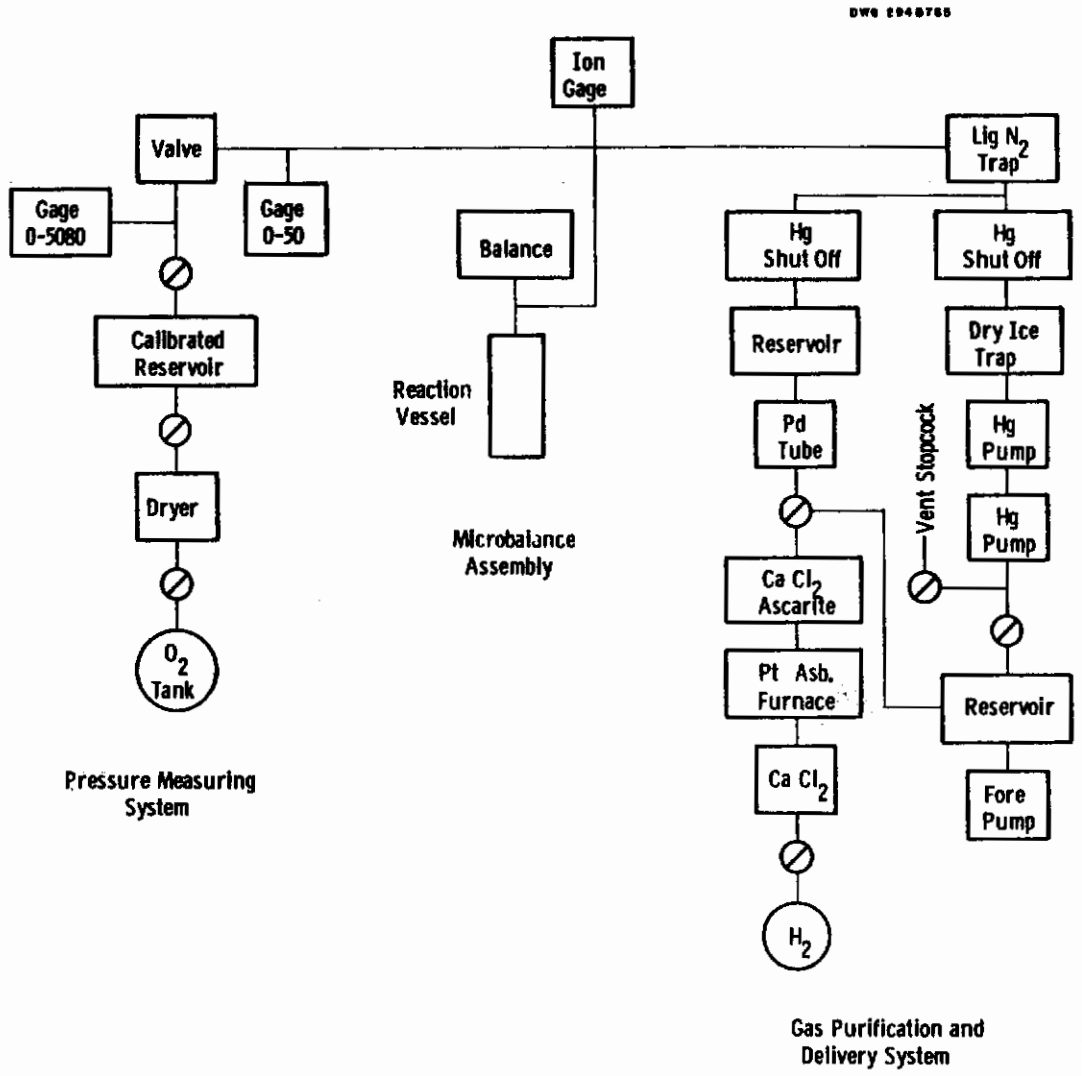

Fig. 2 --Schematic diagram of reaction system

of the apparatus is shown in Figure 3. Oxygen consumed in the reaction is determined by measuring the rate at which the pressure of a calibrated 150 cc reservoir decreases as oxygen is leaked into the reaction system to make up for the oxygen used by the reaction. The leak valve was purchased from the Granville-Phillip Co. of Pullman, Washington. The pressure change of a 150 cc reservoir is measured directly in mm of Hg (Torr). The weight of oxygen used is calculated from the gas laws.

The major difficulty with the method is that no distinction can be made between oxygen consumed to form an oxide film, oxygen consumed to form the volatile oxide or oxygen absorbed by the furnace tube. Using a combination of weight change and oxygen consumption measurements enables one to completely describe the reaction.

3. Furnace Tubes

The furnace tubes were 1 inch outside diameter high purity vacuum tight alumina and purchased from McDanel Porcelain Company of Beaver Falls, Pennsylvania. The tubes were closed at one end and attached to the vacuum system by means of a flange and a rubber O ring. The balance housing and furnace tube details are shown in Figure 4.

One major difficulty was found in using ceramic furnace tubes for tungsten oxidation studies. Alumina was found to react with tungsten trioxide vapor as shown by discoloration of the tube and subsequent cracking. Figure 5 shows cross section photographs of a furnace tube after reaction with tungsten trioxide. The photographs were taken at 4 and 30X. At 1600° the furnace tubes crack after exposure to tungsten trioxide vapors for 10 to 15 minutes. As a result only 1 to 2 experiments can be made on a given ceramic tube. The cracks are at the hot zone of the furnace tube. At lower temperatures the tubes have a longer life but cracking occurs at all temperatures used in this work.

4. Kanthal-Super Furnace for 1600°C

Silicon carbide furnace elements and platinum wound furnaces are usually used for achieving temperatures in the range of 1200°C to 1500°C. Silicon carbide furnace elements can be used above 1500°C but their life is low. Platinum alloys with rhodium also can be used for furnaces above 1500°C. With the development of Kanthal-Super, furnaces can be made to operate at 1600°C for long periods of time.

Kanthal-Super is chiefly molybdenum disilicide with a binder. Kanthal-Super is produced according to powder metallurgical processes in the form of rods of circular cross section. When heated these rods can be formed into suitable hairpin-shaped heating elements.

The specific resistance of Kanthal-Super is low and increases rapidly with temperature. For the 6 mm diameter elements a current of 125 to 130 amperes is required for a 1600°C operating temperature. Since the material is brittle and of low impact strength below 1100°C, it is recommended to keep the furnace above 1000°C or at 1/2 of its operating voltage.

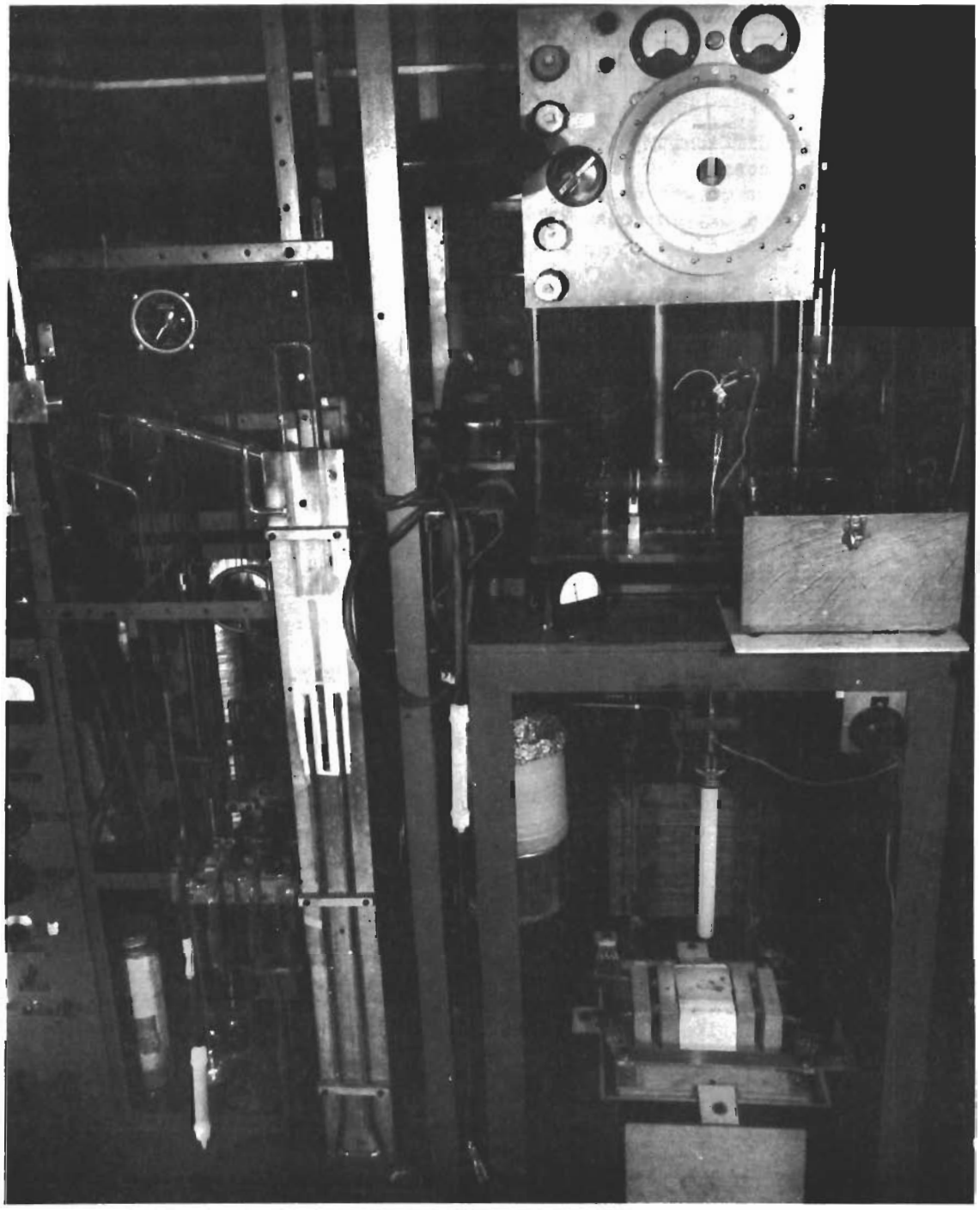

Fig. 3— Pressure measuring device

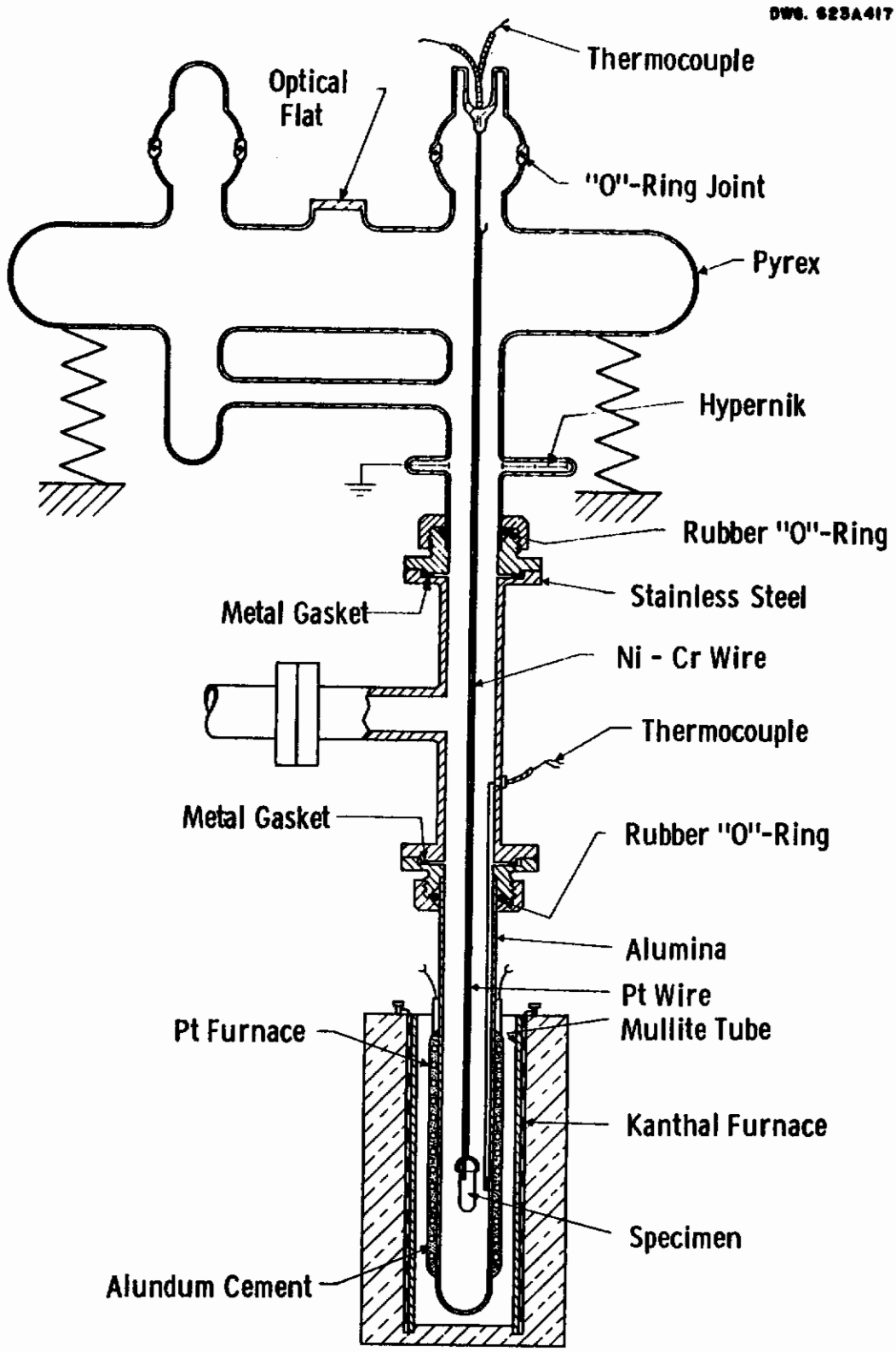

Fig. 4—Reaction system assembly

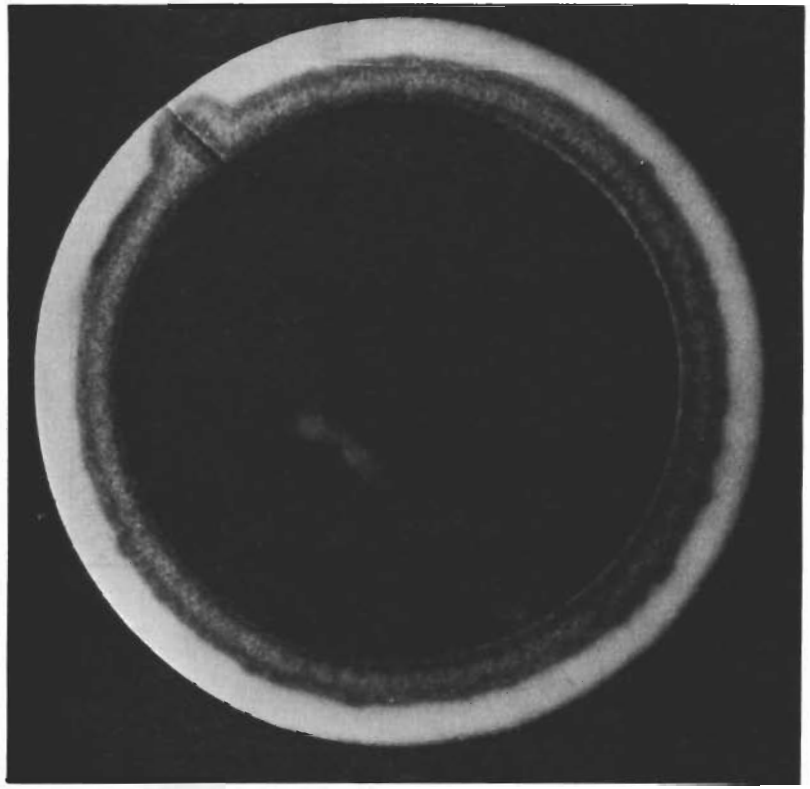

4X

A. Cross-Section of Entire Tube

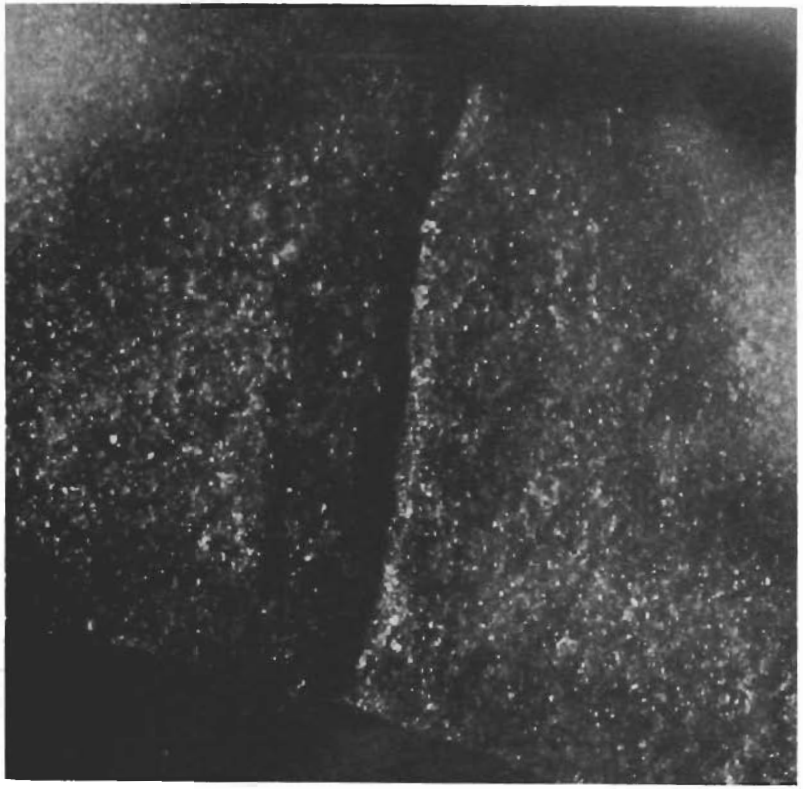

30X

B. Cross-Section of Crack Area

Fig. 5— Reaction of tungsten oxide with alumina and resulting crack

Figure 6 shows a schematic drawing of the furnace and furnace elements while Figure 7 shows a photograph of the furnace and furnace element support. The furnace is 10-1/2 inches square and 13 inches high. The hot space is 2 inches square and 6 inches long. Two S-306 Kanthal-Super elements operating at temperatures up to 1700°C are used to heat the furnace. K-33 brick is used to enclose the hot space. This brick can be used to 1815°C. To lower the heat losses K-30 brick is used on the outside. The Kanthal-Super elements are freely suspended in the hot zone. The power consumed at 1600°C was 1300 watts.

5. Temperature Measurement

Temperatures were measured using Pt - Pt + 10% Rh thermocouples. The thermocouples were calibrated at seven points between 400° and 1200°C. Temperatures above 1200°C were determined by extrapolation of the calibration curve.

Using the balance it was impossible to measure the sample temperature directly. For measurement using the balance the temperature was measured by a thermocouple placed inside the ceramic tube near the sample. When the oxygen consumption method was used alone the thermocouple was mounted directly on the specimen. Comparison was made between the temperatures on the specimen and at a point in the furnace tube near the specimen. All temperatures were corrected to the temperature at the specimen. The thermocouple arrangement is shown in Figure 4.

6. Specimens and Analyses

Specimens were machined from pure tungsten rod. They weigh about 0.825 grams and have a surface area of 0.680 cm^2. These specimens have a dumbbell shape with hemispherical ends. Sharp edges were avoided. The smaller diameter of the dumbbell shaped specimens was used for supporting the specimen by using a loop of platinum wire.

A spectrographic analysis of the tungsten showed the following in parts per million: Si, 1; Ti, <100; Mn, <4; Sb, <10; Fe, 8; Pb, <4; Mg, <1; Al, 1; Ni, 4; Be, <1; Sn, <4; Cu, 1; Ag, <1; Zn, <10; Co, <10; Cr, <4; Ca, 1; B, <4; Nb, <100; Mo, <100; V, <100; Cd, <4. An unreacted specimen is shown in Figure 8A.

7. Specimen Preparation and Pretreatment

The pure tungsten samples were machined from rods that had previously been centerless ground. After the samples were machined, they were polished through 4/0 polishing paper and washed in petroleum ether and pure ethyl alcohol. When only pressure device measurements were made, the samples were suspended from a glass hook in the top of the balance chamber as shown in Figure 4.

Between successive experiments it was necessary to bake the ceramic tube for about twenty minutes at the temperature of the next planned experiment or slightly above. This was necessary to avoid reaction between the clean tungsten sample and oxygen released from the tube during the heat-up of the specimen. Absorbed WO_3 vapor was also expelled from the tube walls during this tube pretreatment.

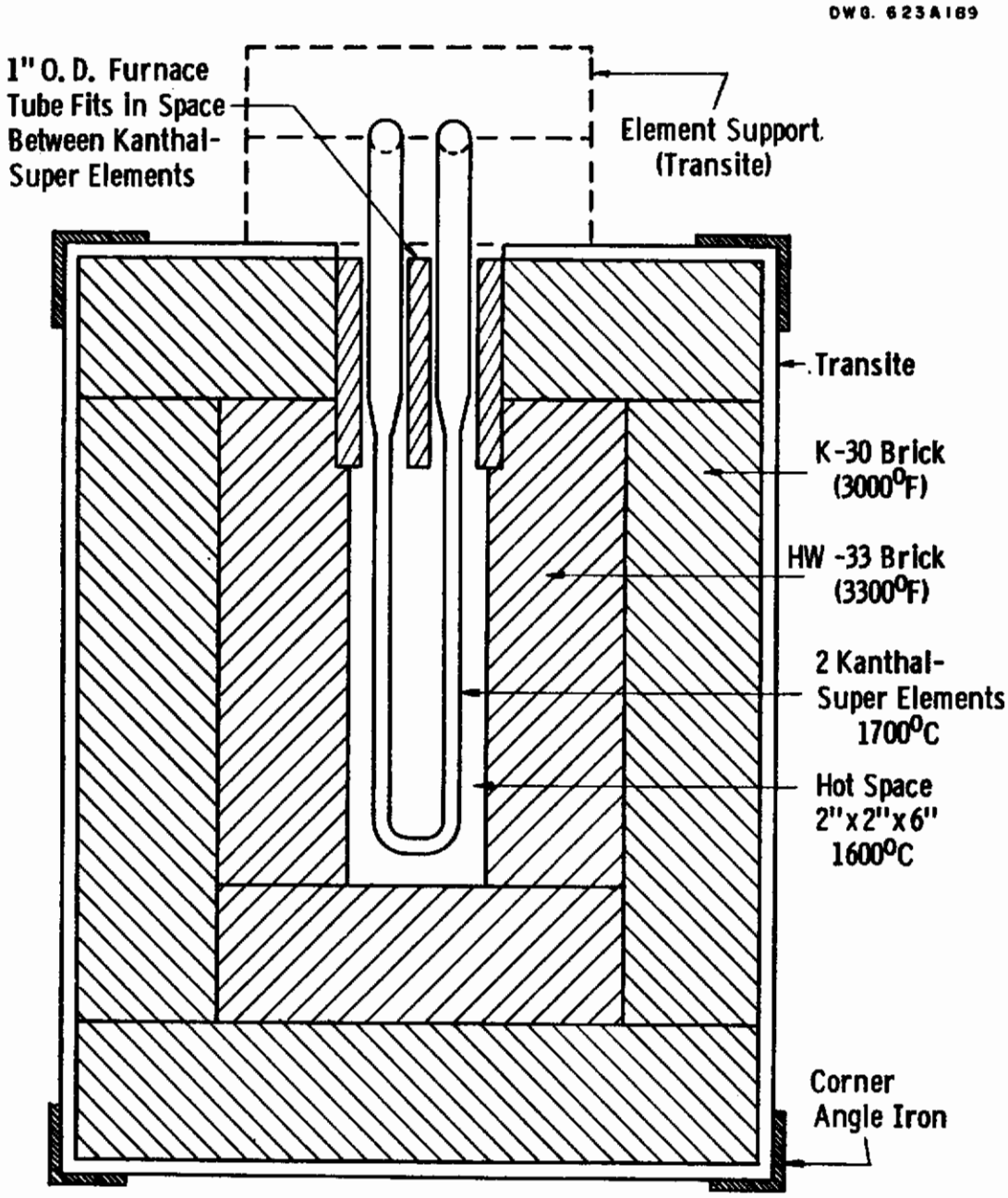

Fig. 6—Kanthal-super furnace (1600°C), 10½" x 10½" x 13"
Maximum power 1760 watts

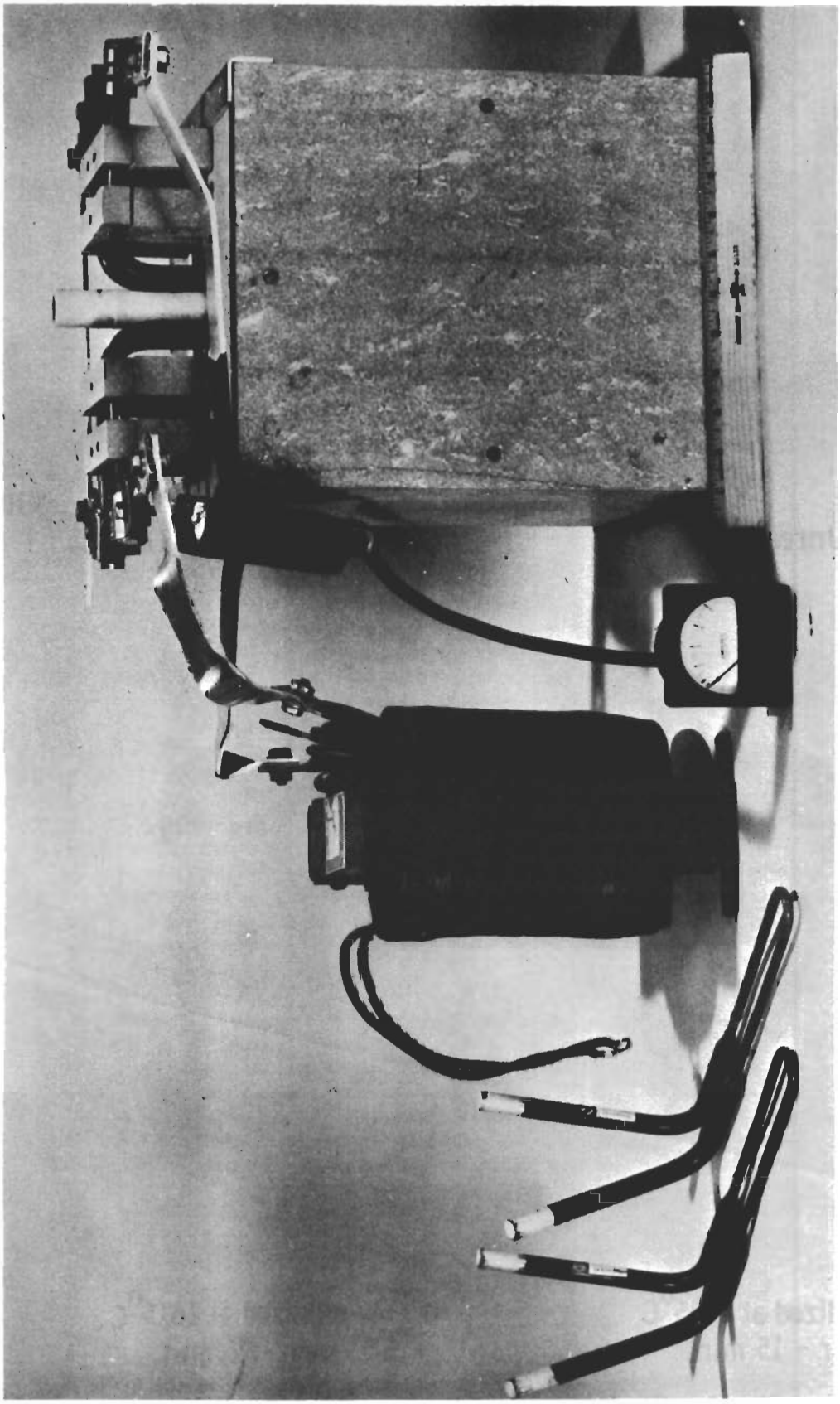

Fig. 7—Kanthal furnace

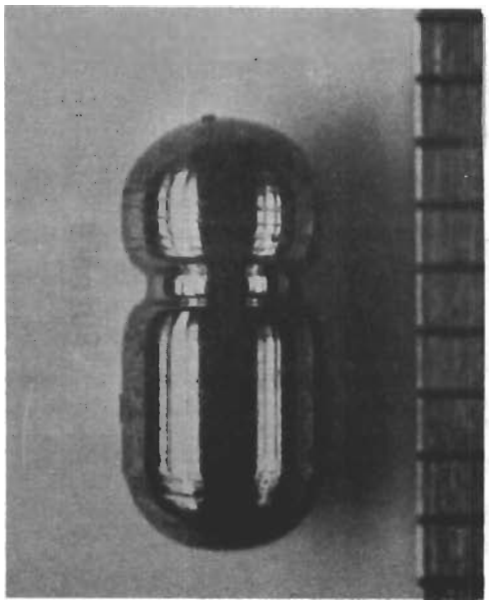

10X

A. Unreacted W

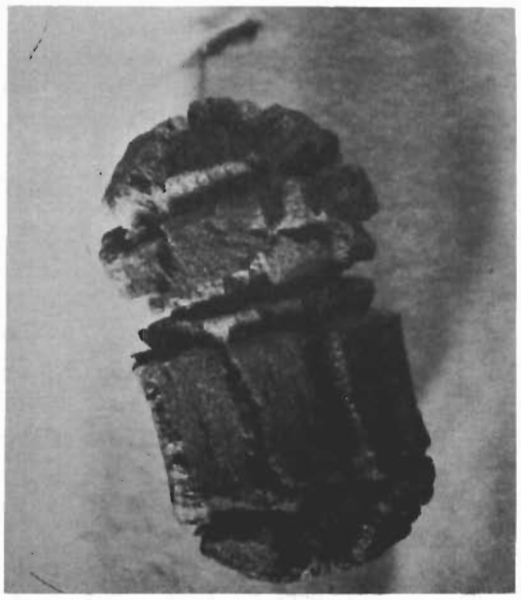

10X

B. W oxidized at 1150°C
5 torr - 2 hr.

10X

C. W oxidized at 1465°C
5 torr - 15 min.

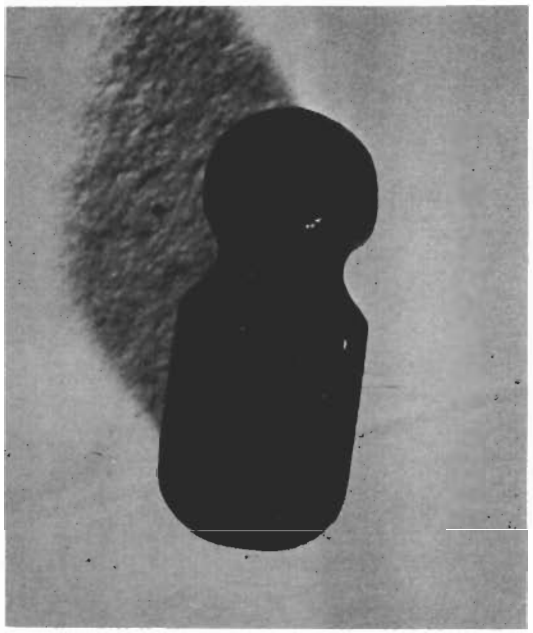

10X

D. W oxidized at 1615°C
5 torr - 15 min.

Fig. 8— Photographs of tungsten specimens

8. Performance of Furnace Tubes and Vacuum System

The performance of furnace tubes at temperatures up to 1175°C was discussed in an earlier paper by Gulbransen and Andrew[3]. Two criteria were used. These were (1) the actual pressure achieved at a given temperature after pumping for a definite period of time, (2) the apparent leak rate of gases into the closed reaction system in units of cm^3 sec^{-1} NTP.

Table 1 shows the performance of a typical alumina furnace tube for temperatures between room temperature and 1600°C. If the gas accumulating in the reaction system volume of 2.6 liters was considered to be 20% by volume of oxygen, an estimate can be made of the oxygen gas building up in the system. These calculations are shown in Table 1.

TABLE 1

Performance of Alumina Furnace Tube as Function of Temperature

Temp. °C	Initial Press.(Torr)	Apparent Leak Rate cm^3 sec^{-1} NTP	Oxygen Equivalent at 20% of gas gm sec^{-1}
R.T.	1×10^{-6}	1.487×10^{-7}	0.385×10^{-10}
1400	1×10^{-5}	7.18×10^{-7}	1.86×10^{-10}
1500	1×10^{-5}	14.87×10^{-7}	3.85×10^{-10}
1600	8×10^{-5}	9.84×10^{-6}	2.55×10^{-9}

9. Method

Experiments were run using the Invar microbalance in combination with the pressure measuring device. In runs in which the weight changes went beyond the limits of the balance, the pressure apparatus alone was used.

After the specimen was brought to temperature, pure oxygen was admitted to the system from a precharged reservoir to the desired pressure. Weight changes were observed with a micrometer microscope as a function of time. Pressure changes in the reservoir were also noted as a function of time by means of a Wallace and Tiernan pressure gauge. A leak valve was used to maintain the pressure in the reaction system. Further experimental details can be found in WADC report TR 59-575 Part II.

RESULTS

1. Classification of Oxidation Phenomena

The results of this and earlier studies may be confusing unless the various phenomena associated with oxidation are systematized. Four basic types of oxidation phenomena occur. (1) Below 500°C oxidation results in the formation of

an oxide film or scale which adheres to the metal. There is no evaporation of tungsten trioxide. (2) Between 600° and 900°C oxide scales form. Large cracks appear in the oxide. Edge type of reaction is prevalent. Evaporation of tungsten trioxide is negligible. (3) Between 950°C and 1250°C oxide scale is formed with large cracks. Evaporation of tungsten trioxide also occurs which makes an analysis of the oxidation data difficult. (4) Above 1250°C oxidation occurs without formation of an appreciable oxide film or scale. Evaporation of tungsten trioxide occurs as rapidly as it is formed.

This study will be concerned largely with type 4 oxidation. It is essential to first consider just the basic facts differentiating types 3 and 4.

2. Type 3 Oxidation

Figure 9 shows a typical oxidation curve for tungsten at 1150°C and 19 Torr oxygen pressure. Curve A shows the oxidation consumption measurements while curve B shows the weight loss measurements using the balance. Both measurements are plotted in mg/cm^2 versus time in minutes. Using curves A and B the actual oxygen in the oxide scale and the tungsten lost by evaporation can be estimated. Curve C shows the calculated oxygen in the oxide scale. 90% of the oxygen reacting remains as oxide scale on the metal.

To relate the weight gain in mg/cm^2 to oxide thickness in Ångstroms, a factor of 67,500 was used. This factor was calculated assuming a density of 7.16 for tungsten trioxide and a surface roughness ratio of unity. These calculations have three limitations: (1) the surface area changes, (2) cracking in the oxide may occur and (3) lower oxides may form. Calculations on Figure 9 show a thickness of 6.75×10^6 Å or 0.675 mm.

Figure 8B shows a photograph of a specimen oxidized at 1150°C and 5 Torr oxygen pressure. Although rounded cylindrical specimens were used, large cracks developed in the oxide scale.

Curve A of Figure 9 can be used to calculate the weight of tungsten reacting and the surface recession rate. Surface recession is defined as the decrease in the dimension of the object as reaction proceeds. The weight of tungsten reacting is calculated by multiplying the weight of oxygen used by the factor 3.83. This assumes the oxide is tungsten trioxide. The surface recession in Ångstroms is related to the oxygen reacted in mg/cm^2 by the factor 198.4.

Another interesting calculation is to compare the actual value of tungsten trioxide evaporating with the theoretical value for a vacuum. Vapor pressure studies of tungsten trioxide in WADC TR 59-575 Part I were used to calculate the theoretical value. Table 2 shows a comparison of the actual weight loss to the theoretical value. The result is given as a percentage of the theoretical value. A percentage of 1.8 was calculated.

3. Type 4 Oxidation

Figure 10 shows both oxygen consumption and tungsten weight loss curves for the reaction at 1250°C and 38 Torr oxygen pressure. Figure 10 also includes the results of the calculated weight losses of tungsten based on the oxygen consumption curves. The agreement of the calculated values with the weight loss

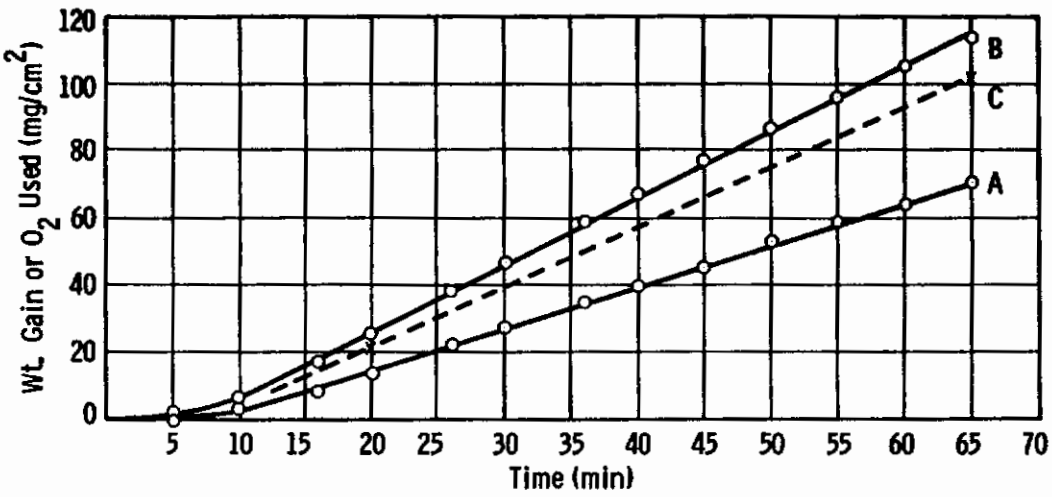

Fig. 9 — Oxidation of tungsten, 1150°C-19 torr
A-Balance, B-O_2 used, C-calculated oxygen in oxide film 103-2

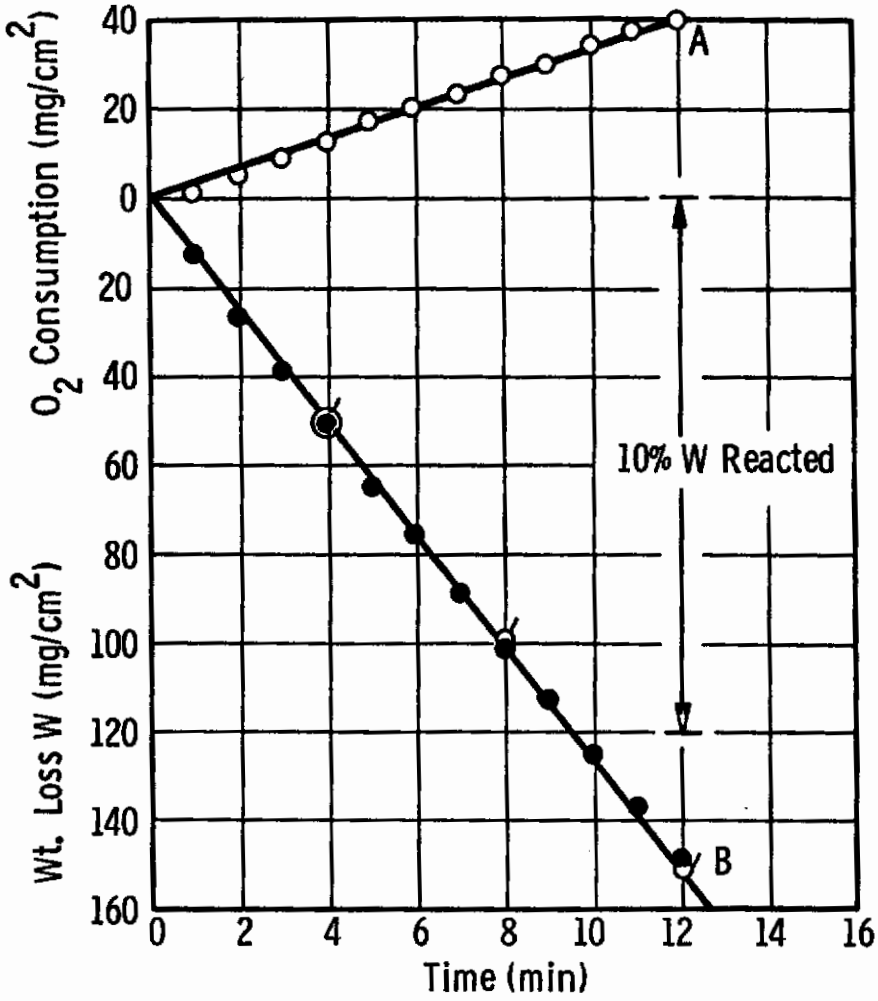

Fig. 10— Oxidation of tungsten

1250^0C-38 torr O_2

- o O_2 consumed - A
- ● Wt. loss balance - B
- ◌ Calculated wt. loss from O_2 consumed

measurements supports the direct use of the oxygen consumption measurements to calculate surface recession rates. The type of calculations made for Figure 9 can be applied directly to Figure 10.

Figure 11 shows an oxygen consumption curve for the reaction at 1615°C and 19 Torr oxygen pressure. Figure 11 also includes a weight loss curve calculated from the oxygen consumption curve. Since the surface area of the cylindrical specimen is changing rapidly, calculations on the surface recession are more complicated but they can be made. These will not be presented here.

Table 2 shows a comparison of the theoretical weight loss values with the experimental values found for the 1250° and 1615°C experiments. At 1615°C the percentage of theoretical was 0.0026. This analysis suggests that vaporization of tungsten trioxide was not the rate controlling mechanism for this temperature range.

The agreement of the experimental weight loss curves with values calculated from oxygen consumption measurements establishes the following basic facts about the oxidation mechanism above 1250°C: (1) tungsten trioxide is formed directly in the reaction and (2) tungsten trioxide evaporates as fast as it is formed.

The transition between type 3 and type 4 oxidation was not sharp and was a function of temperature and pressure. The transition conditions must be established before weight loss curves could be calculated from oxygen consumption data.

TABLE 2

Comparison of Actual Tungstic Oxide Loss With Theoretical Value in Vacuum

Experimental Conditions			Weight Loss of W in Time t		Percentage of Theoretical
Temp. °C	Pressure Torr	Time Seconds	Exptl. g/cm^2	Theor. g/cm^2	
1150	19	3900	0.044	2.411	1.8
1250	38	720	0.150	6.53	2.1
1615	19	480	0.340	12890	0.0026

4. Effect of Temperature

Figures 12, 13, 14 and 15 show the effect of temperature on the oxidation of tungsten for four pressures, 5, 19, 38 and 100 Torr oxygen pressure. The measurements cover the temperature range of 1250° to 1615°C. Due to the rapid reaction rates observed the longest reaction time was 15 minutes. The curves show the rate of oxidation in terms of weight loss of tungsten. Except for the very fast reactions at the highest temperature, the data were taken with both

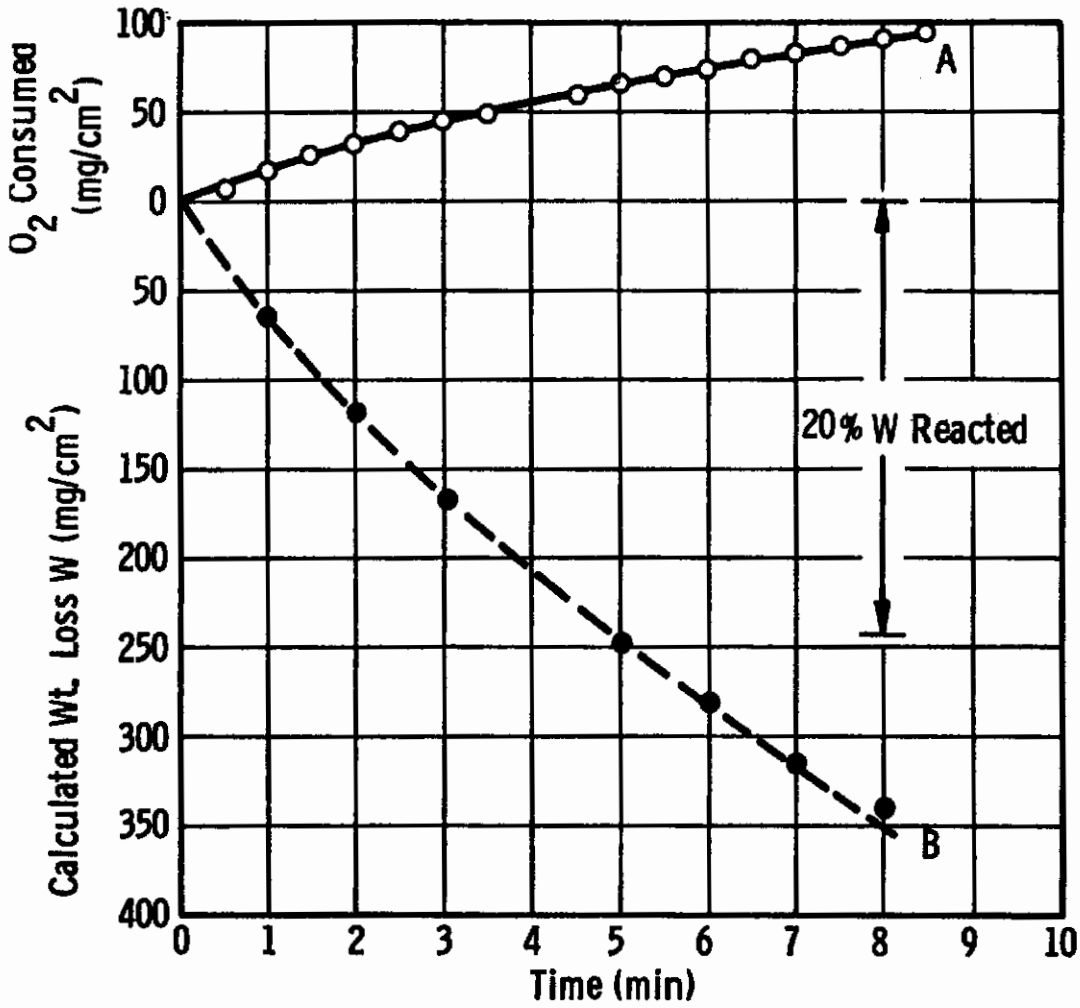

Fig. 11— Oxidation of tungsten

1615^0C-19 torr

- ○ O_2 consumed-- A
- ● Calculated wt. loss from O_2 consumed-- B

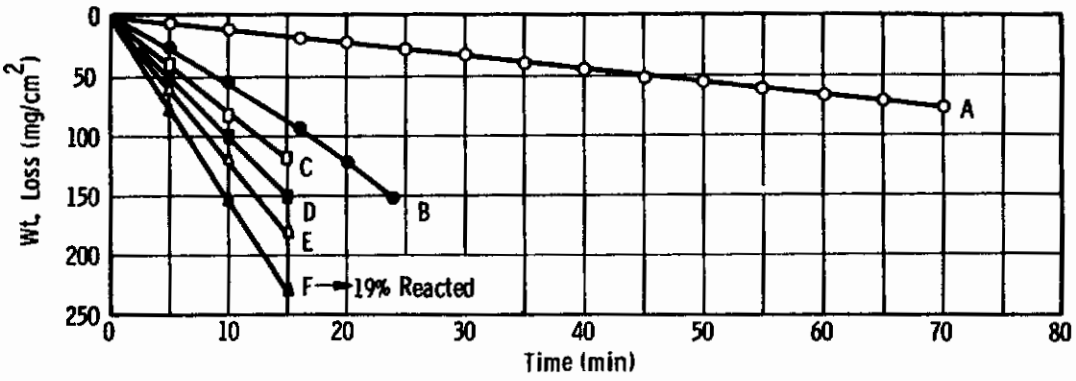

Fig. 12— Effect of temperature on oxidation of tungsten
1150°C-1615°C, 5 torr O_2
A-1150°C, B-1250°C, C-1365°C,
D-1465°C, E-1545°C, F-1615°C

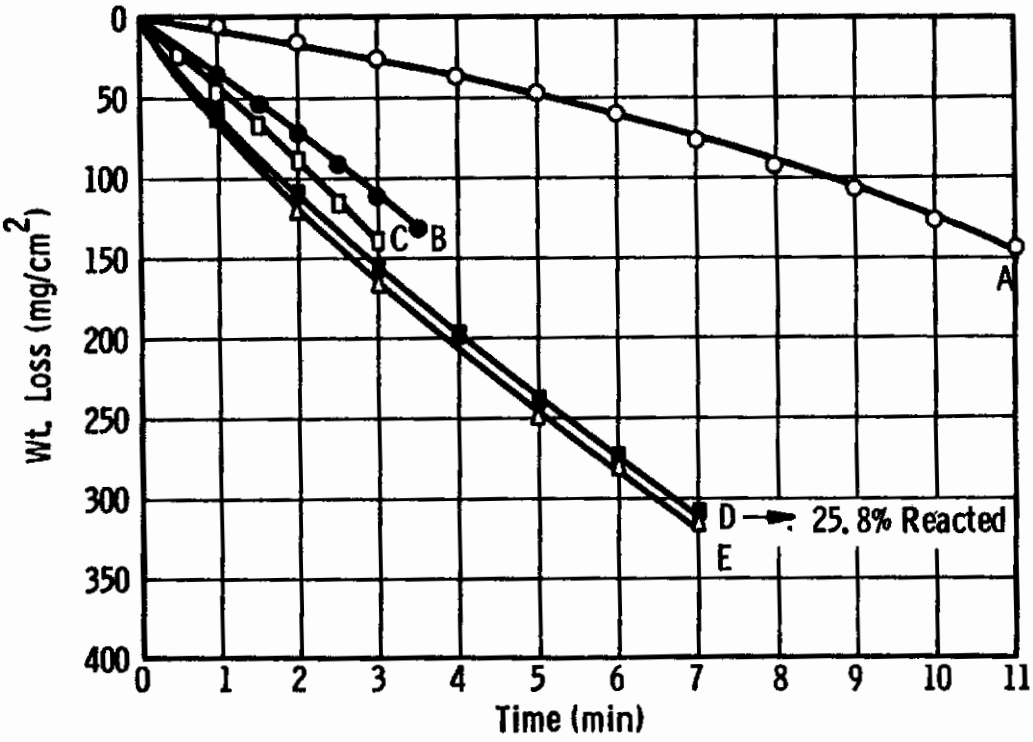

Fig. 13— Effect of temperature on oxidation of tungsten

1250°C-1615°C, 19 torr O_2

A-1250°C, B-1365°C, C-1465°C, D-1520°, E-1615°C

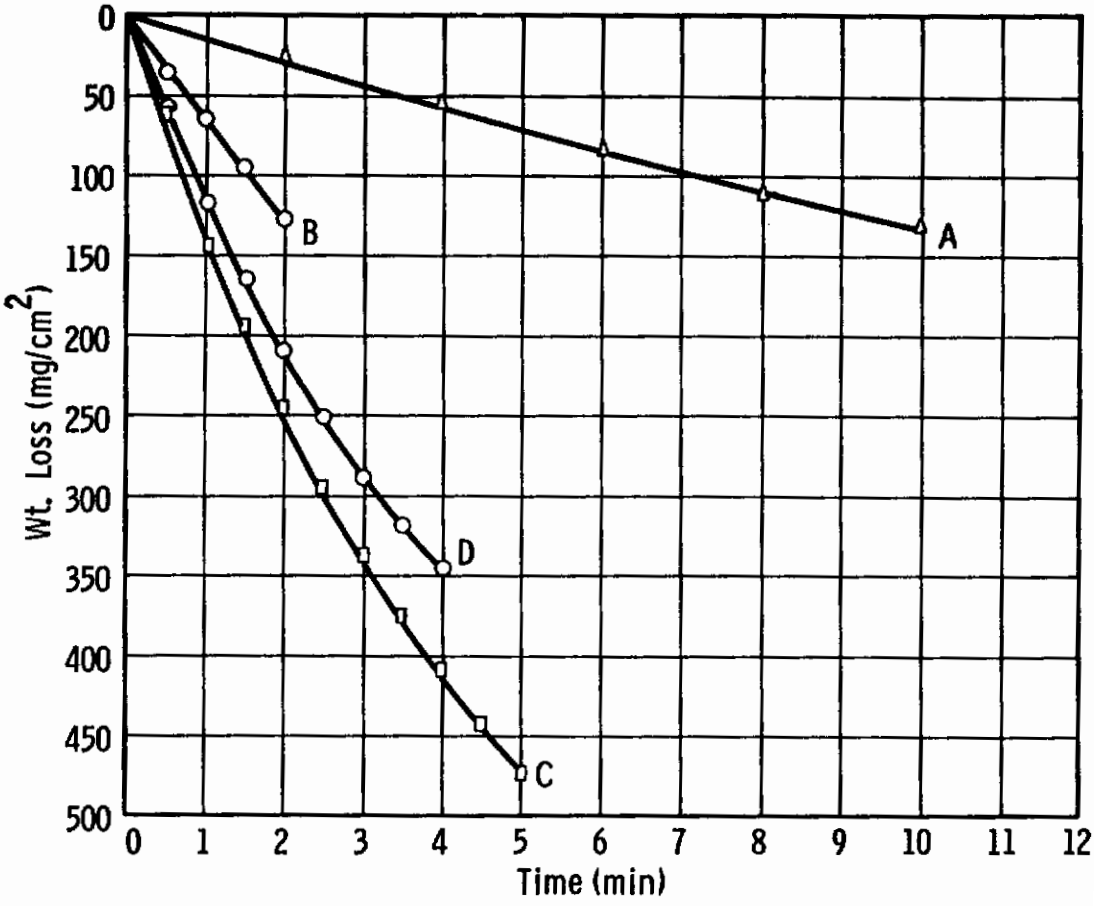

Fig. 14 — Effect of temperature on oxidation of tungsten
1250°-1615°C, 38 torr O_2
A-1250°C, B-1365°C, C-1465°C, D-1615°C

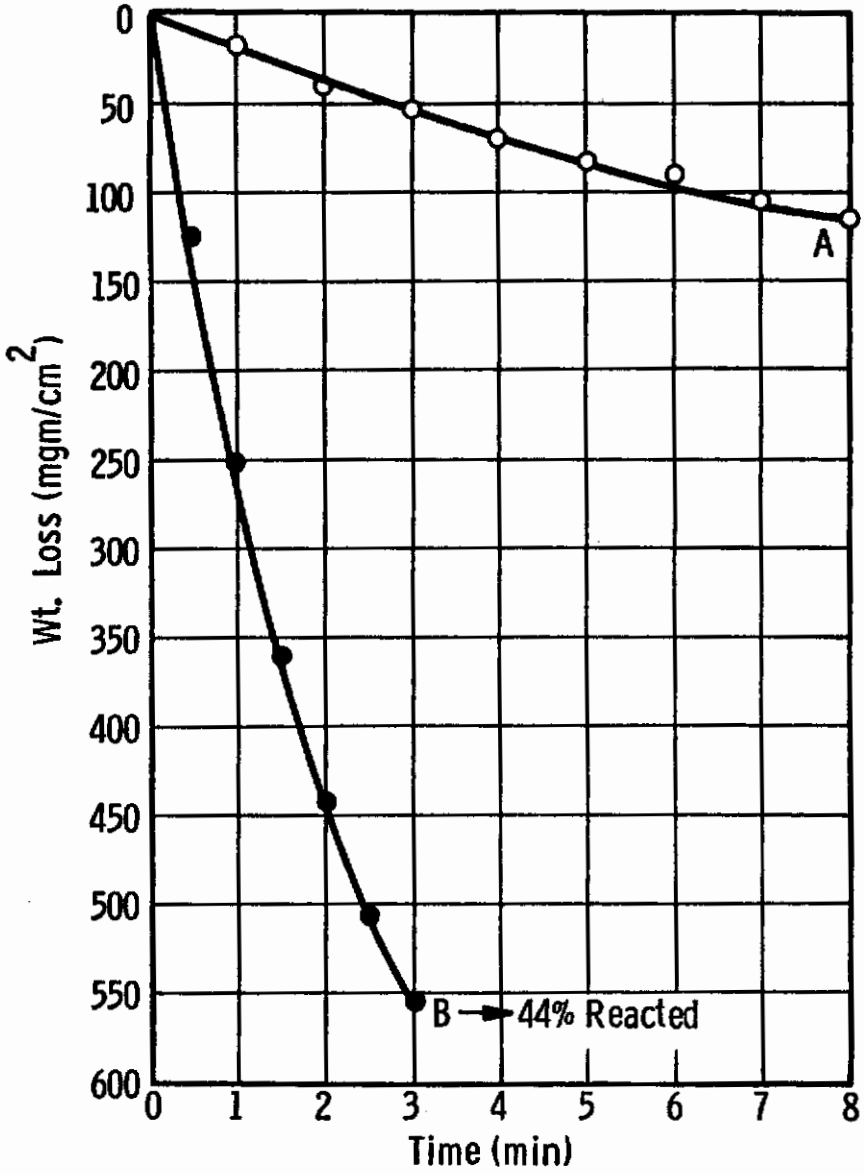

Fig. 15—Effect of temperature on oxidation of tungsten
1250°C-1365°C, 100 torr O_2
A-1250°C, B-1365°C

the Invar beam balance and the oxygen consumption apparatus. For the fast reactions, only oxygen consumption was measured. The tungsten weight loss curves were calculated. All data were calculated on the basis of the original areas of the specimen. The decrease in reaction rate observed with time in Curve B of Figure 15 at 1615°C was directly related to the change in surface area of the specimen.

Figure 8A, B, C and D show photographs of the unreacted and oxidized tungsten specimens. The photographs show the type 4 oxidation phenomena.

Figure 12 shows the effect of temperature for a pressure of 5 Torr. Linear weight loss curves were found at all temperatures between 1250° and 1615°C. The maximum amount of tungsten lost in these experiments was 19% of the original sample weight.

Figures 13, 14 and 15 show the effect of temperature at 18, 38 and 100 Torr oxygen pressures, respectively. Curves A, B and C of Figure 13 were taken with the balance while curves D and E were calculated from the oxygen consumption measurements. A maximum reaction of 27.6% was found for the 1615°C experiment. Curve A shows a different time course for the reaction than curves B, C, D and E. This behavior was noted for all of the experiments at 1250°C at pressures above 5 Torr. A basic change in the reaction mechanism occurs above 1250°C for oxygen pressures greater than 5 Torr.

In Figure 14 curves A and B were taken using the balance while curves C and D were calculated from oxygen consumption data. Curves C and D show an inversion in the rate of reaction with the 1465°C run being faster than the 1615°C runs. Due to the rapid rate of reaction, only two measurements were made at 100 Torr oxygen pressure. Forty-four percent of the sample reacted with oxygen at 1365°C in 3 minutes.

Table 3 shows a summary of the initial rates of tungsten weight loss taken from large scale plots of the data. Figure 16 shows an Arrhenius plot of the data. The rate data are scattered for the high temperature runs due to the high heat rates associated with the reaction. The inversion of the 1465°C and 1615°C runs at 38 Torr are ascribed to the small temperature coefficient for the reaction and to the difficulty of obtaining reproducible results. This inversion would not change the implications of Figure 16 which shows the rate of reaction increases with temperature at all pressures.

The data of Figure 16 were used to estimate a heat of activation of 14,300 cals. per mole. Curves B and D were drawn with the same slopes as A and C. It is noted that the data at 1250°C above 5 Torr oxygen pressure are not consistent with the higher temperature data. This suggests a change in the mechanism of oxidation near 1250°C.

An empirical equation similar to that used by Perkins and Crooks[2] was used to interpret the results.

$$\frac{dw}{dt} = Kp^n e^{-\Delta H/RT}$$

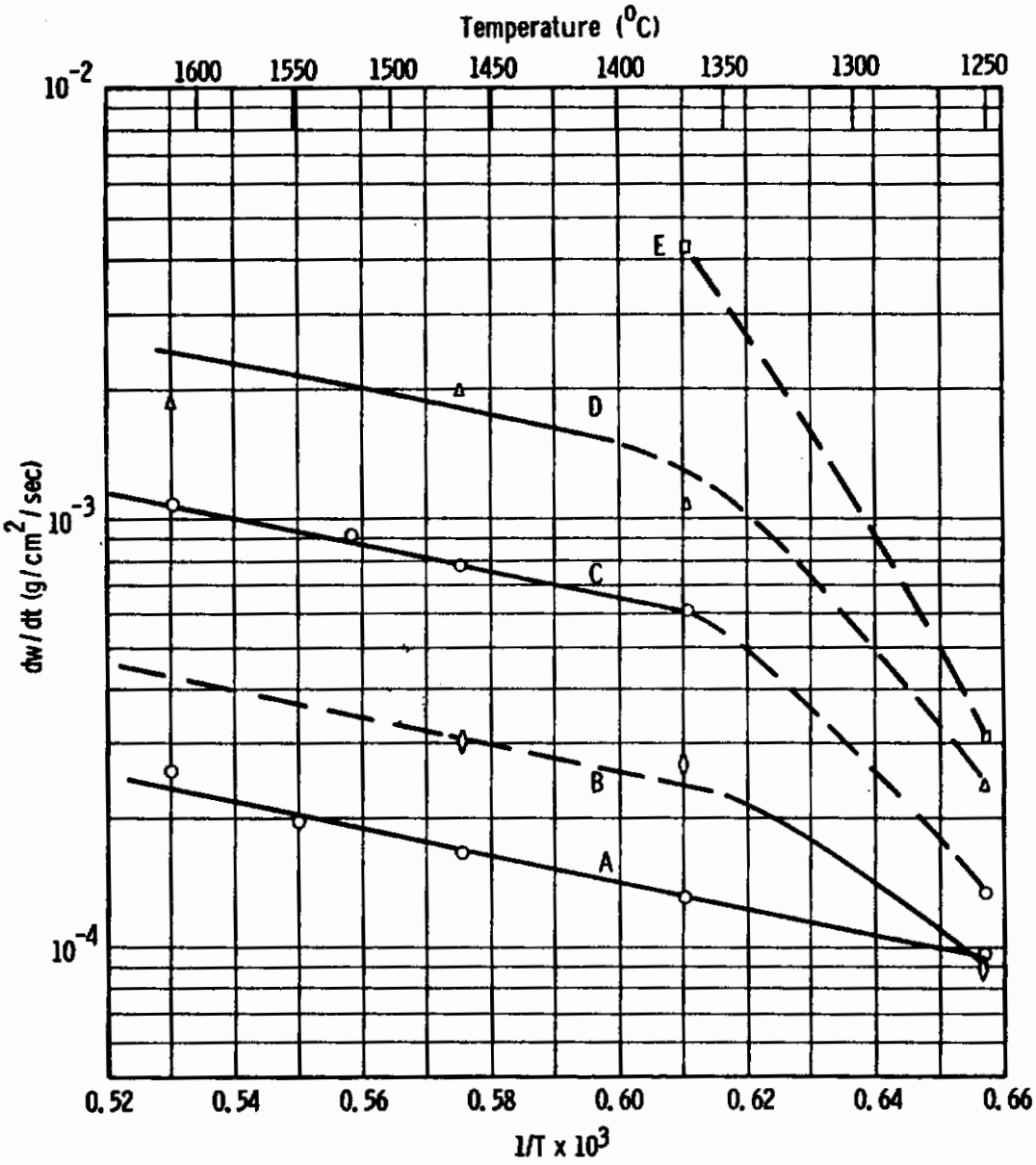

Fig. 16—Log dw/dt vs 1/T 1250°C-1615°C, 5-100 torr of O_2

A-5 torr, B-9.5 torr, C-19 torr, D-38 torr, E-100 torr
ΔH all curves, 14,300 cals/mole

Here $\frac{dw}{dt}$ is the initial rate of tungsten weight loss in units of $g/cm^2/sec$. ΔH is the heat of activation of the rate controlling mechanism in calories per mole. P is the pressure in Torr. T is the absolute temperature. R is the gas constant and K and n are constants. To determine n it is necessary to consider the effect of pressure on the oxidation reaction.

TABLE 3

Summary of Oxidation Kinetics

Temp. °C	$\frac{1}{T} \times 10^4$	Rate ($g/cm^2/sec \times 10^4$) of Weight Change at Pressure (Torr)						
		2	5	9.5	15	19	38	100
1150	7.027	-0.167	-0.189	--	--	+0.208	+0.388	--
1250	6.566	-0.542	-0.972	-1.933	-2.31	-1.33	-2.305	-2.817
1300	6.357	--	--	-2.209	--	-3.66	--	--
1365	6.105	-0.528	-1.32	-2.56	-5.778	-6.14	-10.67	42.52
1400	5.978	--	--	-3.59	--	-5.018	--	--
1465	5.753	-0.703	-1.626	--	-3.83	-7.65	-19.04	--
1520	5.577	--	--	--	--	-9.048	--	--
1545	5.500	--	-1.953	--	--	--	--	--
1615	5.296	--	-2.56	-8.696	--	-10.23	-18.89	--

5. Effect of Pressure

The effect of pressure on the rate of oxidation is shown in Figures 17-21 for temperatures of 1150° to 1615°C. All of the weight loss values were calculated on the basis of the initial surface area of the sample. Figure 17 shows the results at 1150°C for pressures of 2-49 Torr. Pressure has a major influence on the rate of oxidation. For temperatures of 1150°C and higher, pressure is the major factor in determining the kinetics of oxidation. Thus, in Figure 17 a weight gain was observed for the higher oxygen pressures and a weight loss for the lower pressures. Curves D and E are of type 3 oxidation since tungsten trioxide is evaporating from the oxidized sample. Figure 18 shows the results at 1250°C. All of the experiments show a weight loss with the rate of weight loss increasing with oxygen pressure. The oxygen atmosphere was not inhibiting the reaction although the evaporation of WO_3 was probably slowed down. This effect will be discussed later.

Figures 19 and 20 show the results at 1365°C and 1465°C. Nearly linear weight loss curves were observed. Again, the strong effect of pressure was found. Figure 21 shows the results at 1615°C. The decrease in rate of weight loss with time can be related directly to the surface area of the specimen. The trend of the curves in Figure 21 shows the 2 and 5 mm runs are not in line with the general trend of the results. This is due to a lack of reproducibility in temperature of the sample or in the flow of gases in the furnace tube. No change in mechanism should be induced from these two curves.

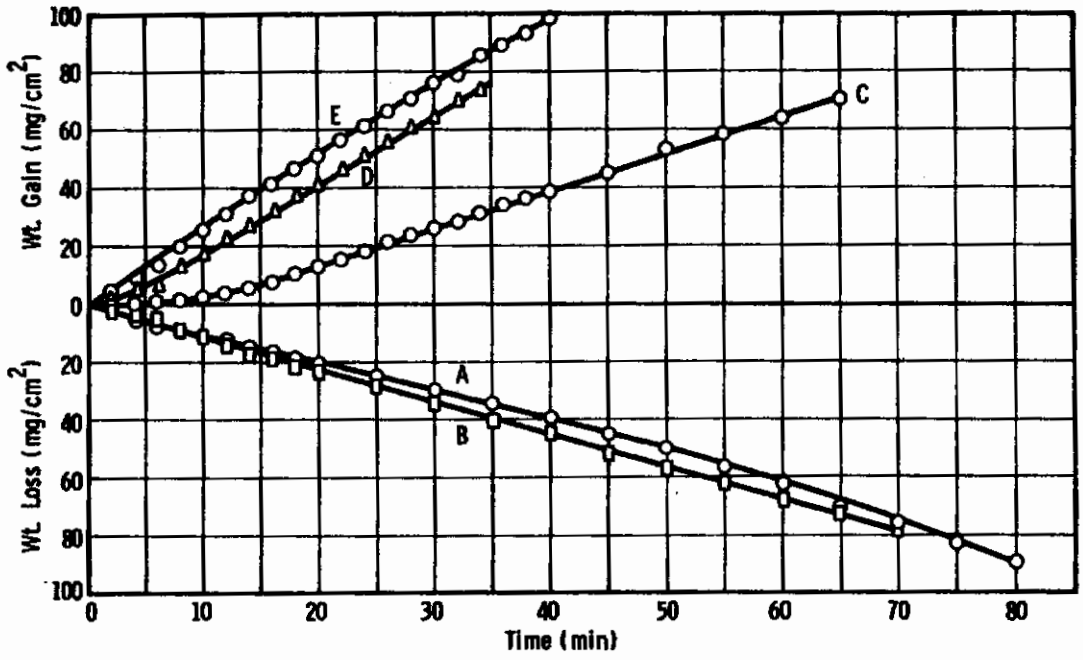

Fig. 17— Effect of pressure oxidation of tungsten
1150°C 2-49 torr oxygen
A-2 torr, B-5 torr, C-19 torr, D-38 torr, E-49 torr

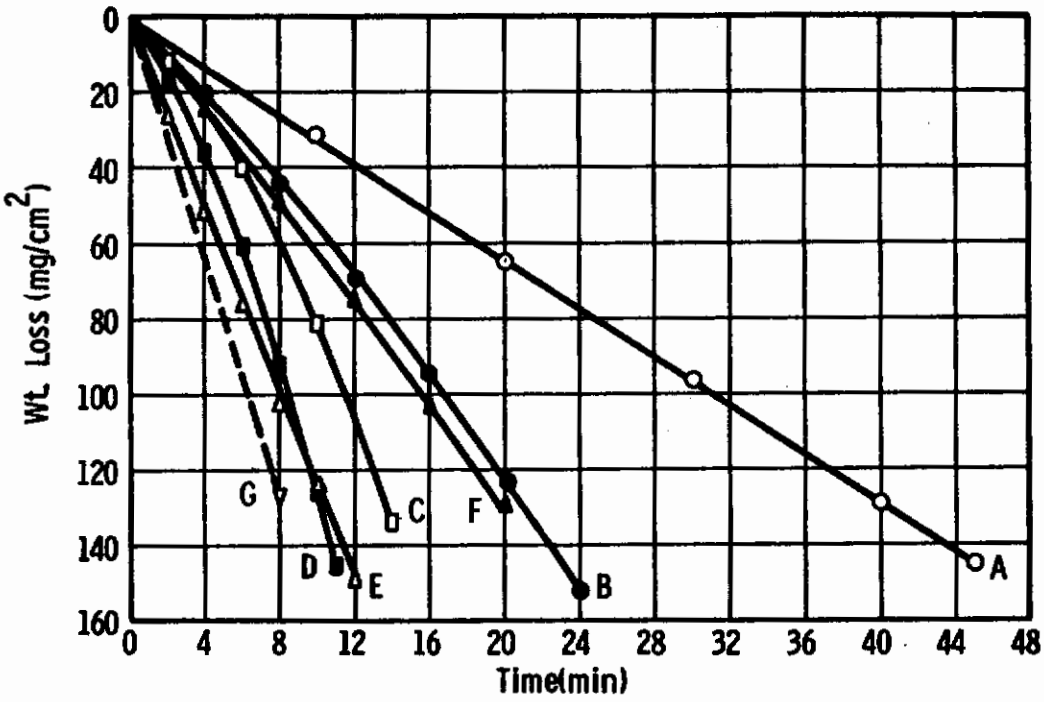

Fig. 18— Effect of pressure on oxidation of tungsten, 1250°C

2-100 torr O_2

A-2 torr, B-5 torr, C-9.5 torr, D-19 torr, E-38 torr,
F-49 torr, G-100 torr

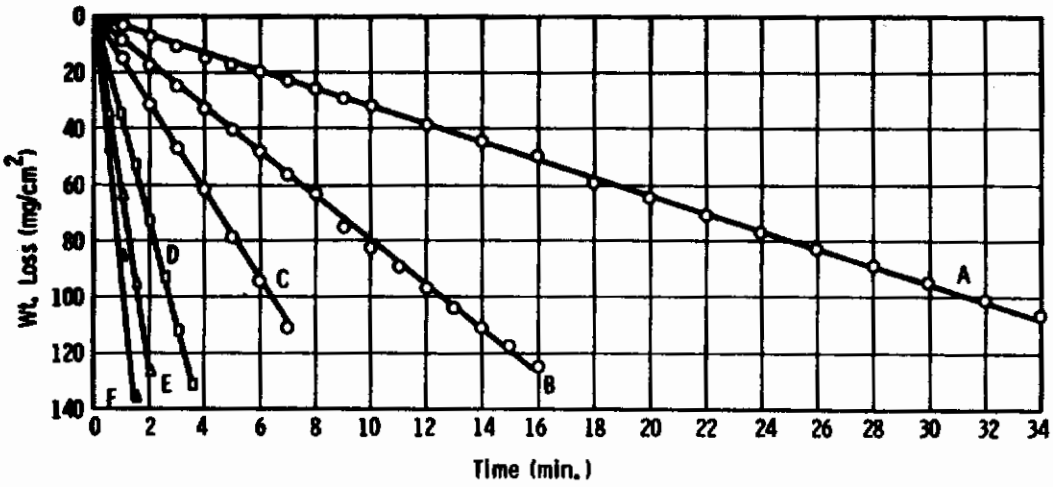

Fig. 19—Effect of pressure on the oxidation of Tungsten. 1365°C - 2 to 49 torr O_2

A - 2 torr; B - 5 torr; C - 9.5 torr; D - 19 torr; E - 38 torr
F - 49 torr

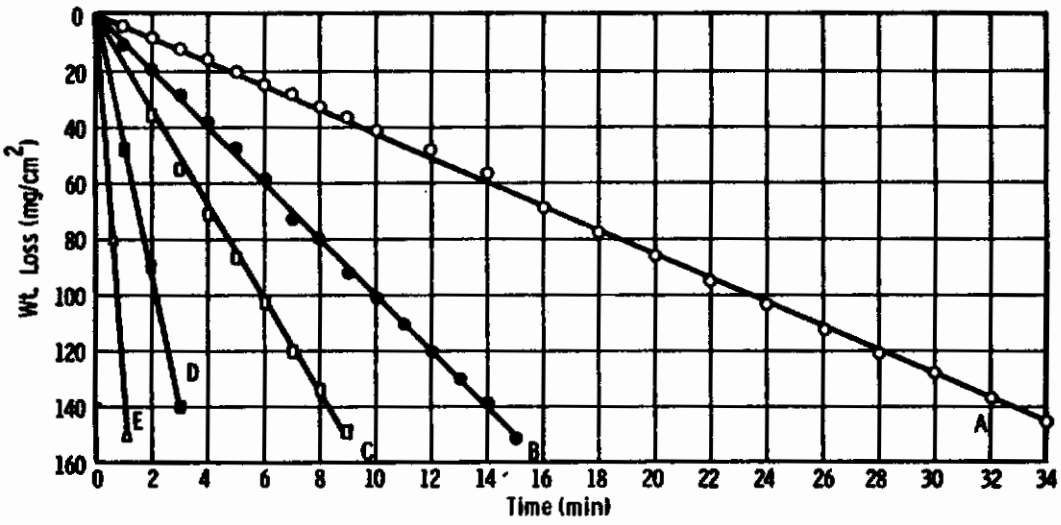

Fig. 20— Effect of pressure on the oxidation of tungsten, 1465°C
2-38 torr O_2
A-2 torr, B-5 torr, C-9.5 torr, D-19 torr, E-38 torr

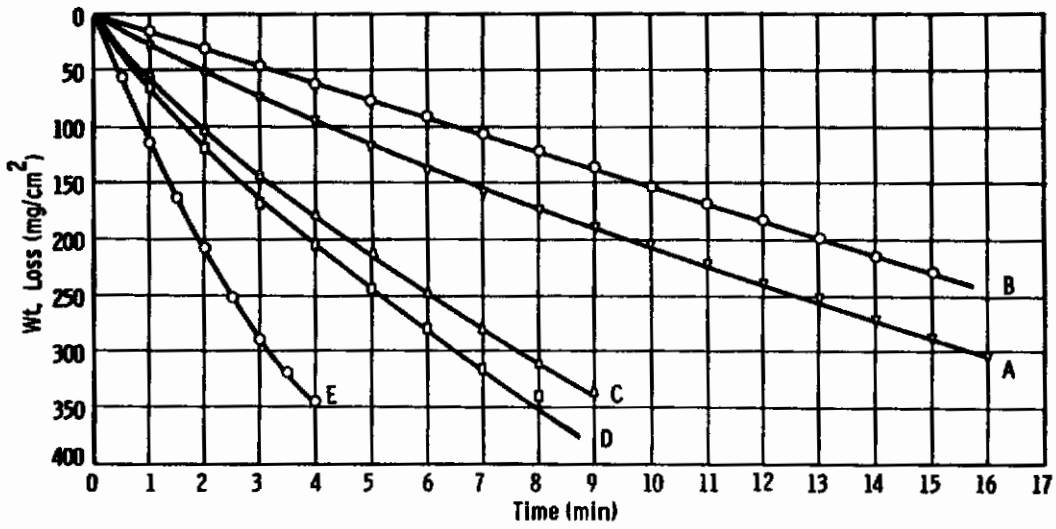

Fig. 21 — Effect of pressure on oxidation of tungsten, 1615°C
A-2 torr, B-5 torr, C-9.5 torr, D-19 torr, E-38 torr

Figure 22 shows the effect of pressure on the initial reaction rate $\frac{dW}{dt}$ on a log $\frac{dW}{dt}$ versus log pressure plot. Four temperatures were considered in Figure 22: 1365°C, 1465°C, 1545°C and 1615°C. The following equation was derived from the data of Figures 16 and 22:

$$\frac{dW}{dt} = 1.87 \times 10^{-3} \; p^{1.122} \; e^{-\frac{14,300}{RT}}$$

This equation fits the results for the temperature range of 1365°C to 1615°C and for pressures of 5 to 38 Torr to about 10% accuracy.

DISCUSSION

1. Summary of Kinetic Work

In the previous part of this report the primary chemical reaction of pure tungsten was studied using cylindrical specimens. Above 1250°C and at pressures up to 38 Torr of oxygen the weight change curves showed no evidence of an initial pickup of oxygen to form an oxide film. This does not eliminate the possibility that an adsorbed oxygen layer is formed since the weight change associated with an adsorbed oxygen monolayer would not be measured using our present methods. The observed weight loss curves were nearly linear with time. For a short period of reaction the data could be fitted to the equation $W = Kt$, where W is the weight loss in milligrams per cm^2, K is a constant and t is the time. For longer periods of time, surface area changes occurred which decreased the rate of weight loss.

The initial rate constant K could be fitted to an exponential function of temperature - i.e. $K = Ze^{-\Delta H/RT}$. A heat of activation of 14,300 calories per mole was found, while the frequency factor Z has the units of grams of tungsten reacting per square centimeter of area per second.

The effect of pressure on the oxidation of tungsten was studied between 1150° and 1615°C. These results could be fitted to the equation $K = ap^{1.122}$ where K is the rate constant, p is the pressure in Torr and a is a constant. The value $p^{1.122}$ suggests that the reaction was nearly a linear function of pressure.

Combining the temperature and pressure rate laws, we have the final empirical rate equation

$$\frac{dW}{dt} = -1.87 \times 10^{-3} \; p^{1.122} \; e^{-\frac{14,300}{RT}} \; t$$

Here $\frac{dW}{dt}$ is the initial rate of reaction in grams per sec. per cm^2 and t is

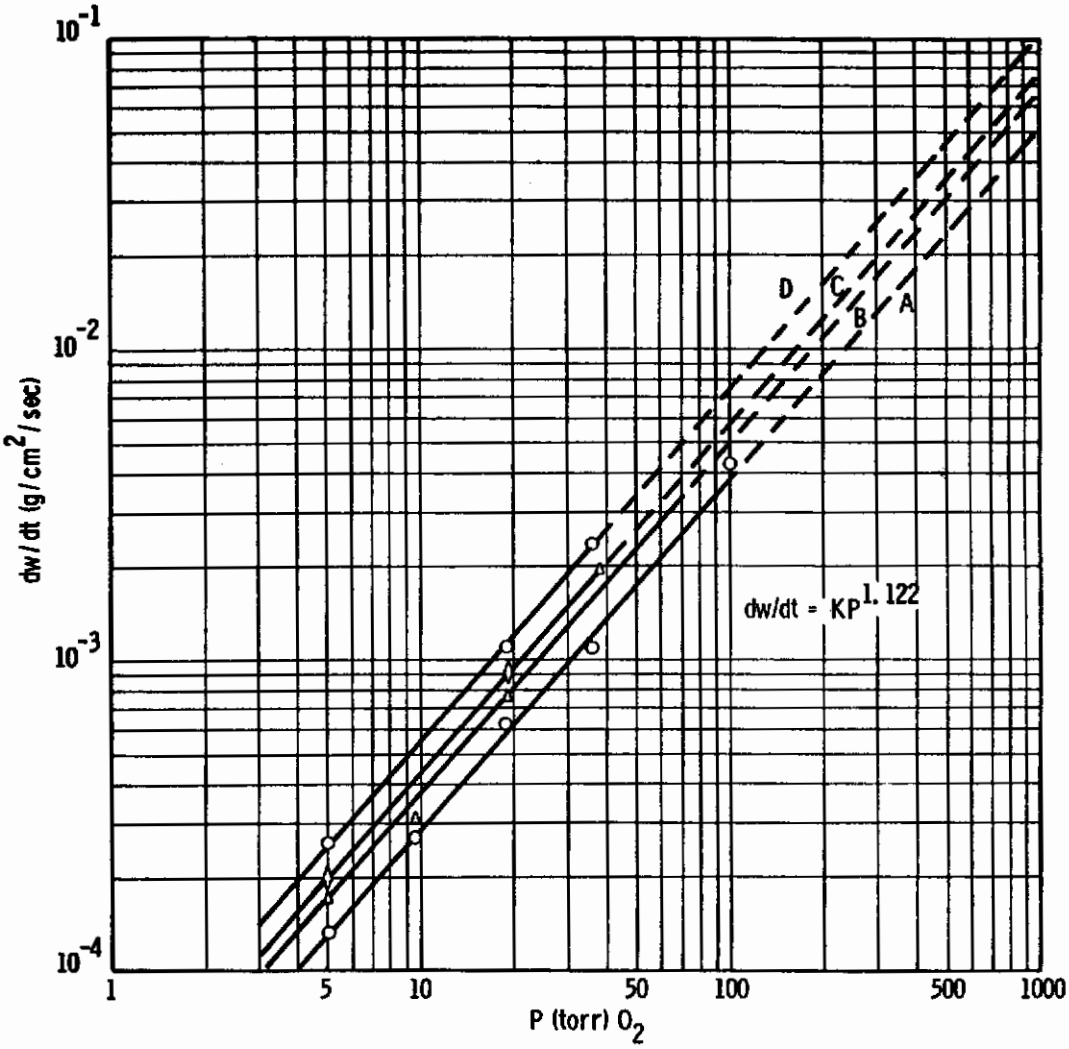

Fig. 22—Effect of pressure on initial rate of oxidation
Log-log plot A-1365°C, B-1465°C, C-1545°C, D-1615°C

the time in sec. In terms of atoms of tungsten reacting we have the equation

$$\frac{dW}{dt} = 6.10 \times 10^{18} \; p^{1.122} \; e^{-\frac{14,300}{RT}} \; t \; .$$

Any proposed mechanism must account for four essential experimental facts: a nearly linear dependence on pressure, a linear time dependence during the initial stages of reaction, an exponential temperature dependence and the absolute value for the rate of reaction as given by the above equations.

A surface reaction may be separated into at least five distinct processes, the slowest of which determines the rate of the reaction:

1. Transport of the reacting gas to the surface
2. Chemisorption of the gas
3. Chemical reaction at the surface
4. Desorption of the reaction products
5. Transport of the reaction products into the bulk phase.

In general processes 1 and 5 are diffusion processes; and if these are rate-controlling, the temperature dependence of the reaction rate may be expected to vary with $T^{1/2}$ where T is the absolute temperature. Further, surface reactions usually have activation energies of 30 kcal per mole while gas diffusion processes have much lower values[4].

2. Temperature Rise of Sample

Due to the rapid oxidation reaction the specimen temperature will increase above the ambient temperature. This can be estimated as follows. Consider a tungsten sample weighing 0.81 gms and having a surface area of 0.68 cm^2 reacting with oxygen at 49 Torr pressure at 1465°C. The experiment shows a weight loss of tungsten of 2.87×10^{-3} g/sec. This is equal to 4.22×10^{-3} g of W/cm^2/sec or 2.30×10^{-5} moles of W/cm^2/sec.

According to WADC TR 59-575 Part II the heat of formation of WO_3, $\Delta H_{f_{WO_3}}$, at 1700°K is - 194.75 kcal/mole of WO_3. From the same report we note the heat of sublimation, $H_{s_{WO_3}}$ at 1500°K is 121 kcal/mole of W_3O_9 or 40.3 kcal/mole of WO_3. If we make a heat balance of the formation and evaporation processes we have $\Delta H_{f_{WO_3}} + \Delta H_{s_{WO_3}} = -154.7$ kcal/mole.

We can now calculate the net heat released at the sample as 2.4 cals/sec. Using the value of heat capacity given by Kubaschewski and Evans[5] for tungsten as 3.81×10^{-2} cal/°C/g we calculate a temperature rise of 63°C/sec. without radiation losses.

To evaluate the temperature rise we need to know the heat losses. At 1400°C the major heat loss is due to radiation. Estimates from data given by McAdams[6] show that natural convection plays a very minor role at 1400°C.

Radiation losses can be evaluated using Planck's equation $h_r = C_r \epsilon (T^4 - Ta^4)$. Here h_r is the heat rate in cals/cm^2/sec, ϵ is the emissivity, $C_r = 1.354 \times 10^{-12}$ cal cm^{-2} deg^{-4} sec^{-1}, T is the sample temperature and T_a is the furnace tube wall temperature.

Since the emissivity of the sample and walls differ we use the following relation to calculate an average emissivity ϵ.

$$\frac{1}{\epsilon} = \frac{1}{\epsilon_1} + \frac{A_1}{A_2}\left[\frac{1}{\epsilon_2} - 1\right]$$

Here $\frac{A_1}{A_2}$ is the ratio of diameters of specimen and tube, ϵ_2 is the emissivity of the ceramic wall and ϵ_1 is the emissivity of the sample. If ϵ_2 is nearly 1 and if $\frac{A_1}{A_2}$ is small the second term becomes small compared to the term $\frac{1}{\epsilon_1}$. For this case $\epsilon \approx \epsilon_1$.

We will calculate the temperature rise for two values of the emissivity i.e. $\epsilon_1 = 1.0$ and 0.50. The first case is when the tungsten sample has a thin film of oxide on the surface while the second case refers to a brighter surface. Using ϵ_1 of 1.00 and $T_a = 1738$°K we calculate a ΔT of 113°C while using a value of ϵ_1 of 0.50 we calculate a ΔT for the sample of 207°C.

Experiments with the thermocouple mounted on the specimen showed temperature increases of 15 to 20°C, much less than those calculated above. The reason for this discrepancy was not clear. Experimentally it was difficult to mount the thermocouple so that the specimen temperature was actually measured. On the other hand, no burnup was observed which suggests that the temperature coefficient of the reaction was small or that the calculated temperature rises were not taking place. The effect of temperature on the rate of oxidation between 1400°C and 1600°C was small which limits the reaction and prevents burnup.

3. Decrease in Surface Recession Rates Above 1800°C

Perkins and Crooks[2] have reported that the rate of weight loss of tungsten in air at 1 to 15 Torr oxygen pressure decreases above 1800°C. These experiments utilize observations on the diameter of rods undergoing reaction. Perkins and Crooks relate this inversion to a thermal dissociation of tungsten trioxide. Two facts suggest that these results must only be accepted with reservations. First, thermochemical calculations based on the data of King et al[7] show that all of the tungsten oxides are stable. Second, Langmuir studied the oxidation reaction for pressures in the micron range where the effect of oxide dissociation would be more readily observed. Using a pressure change method Langmuir's results show no indication of an inversion in the rate of reaction at 1800°C. It would appear that the direct measurement method should be investigated and the results compared to oxygen consumption or weight loss measurements. One explanation for the conflicting results is that surface energy considerations are such that tungsten diffuses to the hot zone where reaction with oxygen occurs. Such a phenomena would cause an error in the direct measurement of reaction rates.

4. Future Work

Several conclusions can be drawn from this work which have a bearing on future extensions of the work. Using conventional alumina furnace tubes, a practical operating limit of 1615°C was found. Tungsten trioxide vapors diffuse into alumina causing cracks to occur. Above 1600°C cracks were found after 10 minutes of exposure to tungsten trioxide. Extremely high heat rates were found for tungsten reacting with oxygen above 1400°C. These heat rates make it difficult to determine the reaction temperature precisely.

To study the kinetics of oxidation above 1615°C will require either direct electrical heating or high frequency heating of the specimen. Micro-comparator and oxygen consumption measurements should be used for measuring the rates of reaction. Several difficulties will arise. These are (1) the end effect when electrical heating is used, (2) measurement of reaction temperature, (3) influence of volatile reaction products on temperature measurement and (4) maintenance of uniform temperature in the reaction system.

The oxygen gauge described in WADC TR 59-575 offers an alternative method for measuring rates of oxidation.

Studies on the rates of oxidation or surface recession should be carried to temperatures approaching the melting point. The effect observed by Perkins and Crooks should be tested thoroughly.

SECTION II. OXIDATION OF 50 W - 50 Ta ALLOY AT TEMPERATURES OF 1068 to 1458°C

INTRODUCTION

In experiments between 800 and 1200°C on the oxidation rate of 90 W - 10 Ta, 75 W - 25 Ta and 50 W - 50 Ta, as reported in WADC TR 59-575 Part II, it was found that the latter alloy offered the greatest resistance to oxidation. It was observed that the tungsten rich alloys oxidized linearly while the 50 W - 50 Ta alloy appeared to form a protective scale. In the latter case there was some question about the shape of the oxidation curve, since it was not possible to correct the balance measurements for possible loss of tungstic oxide gas. Data for the other two alloys were corrected for the vaporization of WO_3.

In the previously reported study, measurements on the vapor pressure over the Ta_2O_5 - WO_3 system indicated that more than 99% of the vapor consisted of tungsten oxide with the principal species W_3O_9 (g). It was found that the solid became richer in tantalum oxide, with a break in the curve occurring at 62 mole percent WO_3. It was suggested that this composition corresponded to a tantalum substituted tungsten oxide, $Ta_{10}W_{80}O_{49}$, which is analogous to the compound $W_{18}O_{49}$. The principal evidence for this suggestion was twofold: an oxygen to metal ratio of 2.730, which is quite close to 2.722 for $W_{18}O_{49}$; and WO_3 pressure in fair agreement with that over $W_{18}O_{49}$, corrected for the entropy of mixing when tantalum is substituted for tungsten. X-ray data were inconclusive for this compound.

The WO_3 pressure over the compound was about 2.5 percent of that over WO_3. Hence, if a protective oxide were formed on the 50 W - 50 Ta alloy, its reduced volatility would increase its protection.

In WADC Technical Report 59-13 by Schmidt, Klopp, Albrecht, Holden, Ogden and Jaffee[8] on tantalum, it was found that the tantalum-tungsten alloys with tantalum present at concentrations above 50% were less oxidation resistant than the 50-50 alloy. These were screening tests where the weight gained after two hours at 1200°C in air was measured. Some lower tungsten alloys of tantalum were studied by Schmidt et al[8] using gravimetric measurements. These indicated that the initial oxidation of 5, 10, and 20% tungsten-tantalum alloys is almost parabolic at 1200°C in air. These same alloys oxidized at a rate which was linear at 1400°C in air.

The purpose of the present study is to measure the rate of oxidation of the 50 W - 50 Ta alloy at high temperatures.

EXPERIMENTAL

The apparatus for this research was described in WADC Technical Report 59-575 Part II. Briefly, it consists of an inductively heated platinum susceptor which heats the sample by radiation. The furnace is a water cooled pyrex tube. Temperature was measured with a platinum-platinum-10% rhodium thermocouple whose shielded leads filter out the r.f. voltage. Effectiveness of the filtering was checked by comparing temperatures measured by an optical pyrometer with thermocouple measurements. Agreement was within the reproducibility of the optical measurements. To measure oxygen consumption by the sample, a known concentration

of oxygen in an oxygen-argon mixture is flowed over the sample and oxygen concentration of the exhaust gas is measured with an oxygen gauge[9]. This gauge uses a heated stabilized zirconia tube as a solid electrolyte in an oxygen concentration cell, where the exhaust gas is compared to a standard. The amount of gas is measured with a flow meter. The e.m.f. of the oxygen gauge is recorded.

Experiments begin by flushing out the system with the argon-oxygen mixture. The sample is brought up to temperature rapidly with both the flow rate and temperature controlled manually. Due to the relatively large volume of the system, a lag of several minutes occurs between the time of the sample reaching temperature and the oxygen gauge reacting to the decreased oxygen concentration.

RESULTS

The data obtained between 1068° and 1458°C were shown in Figure 23. Here the oxygen consumption has been converted to weight of oxygen reacting per cm^2 of sample. These samples were oxidized in 0.2 atm. of oxygen and 0.8 atm. of argon.

To analyze the data we used the general rate equation

$$W^n = at$$

Here W was the weight gain, t was the time and a was a constant. In logarithmic form this equation becomes

$$\log W = \frac{\log a}{n} + \frac{1}{n} \log t$$

or

$$\frac{\log W}{\log t} = \frac{1}{n} + \frac{\log a}{\log t}$$

When n was 1 the reaction was termed linear and was controlled by an interface reaction mechanism. A diffusion controlled reaction gave a value of 2 for n as shown by Wagner and Grünewald[10]. The value of n was found by plotting log W versus log t.

Plots of log W versus log t of all of the data show decreasing slopes for longer time periods. This indicates the values of n given in Table 4 were increasing in value with time. We conclude that the protective properties of the oxide scale were improving.

TABLE 4

Kinetic Data for Oxidation of 50 W - 50 Ta Alloy

Temperature °C	Exponential Constant n
1068	1.8
1217	2.7
1330	2.8
1348	2.2
1458	1.5

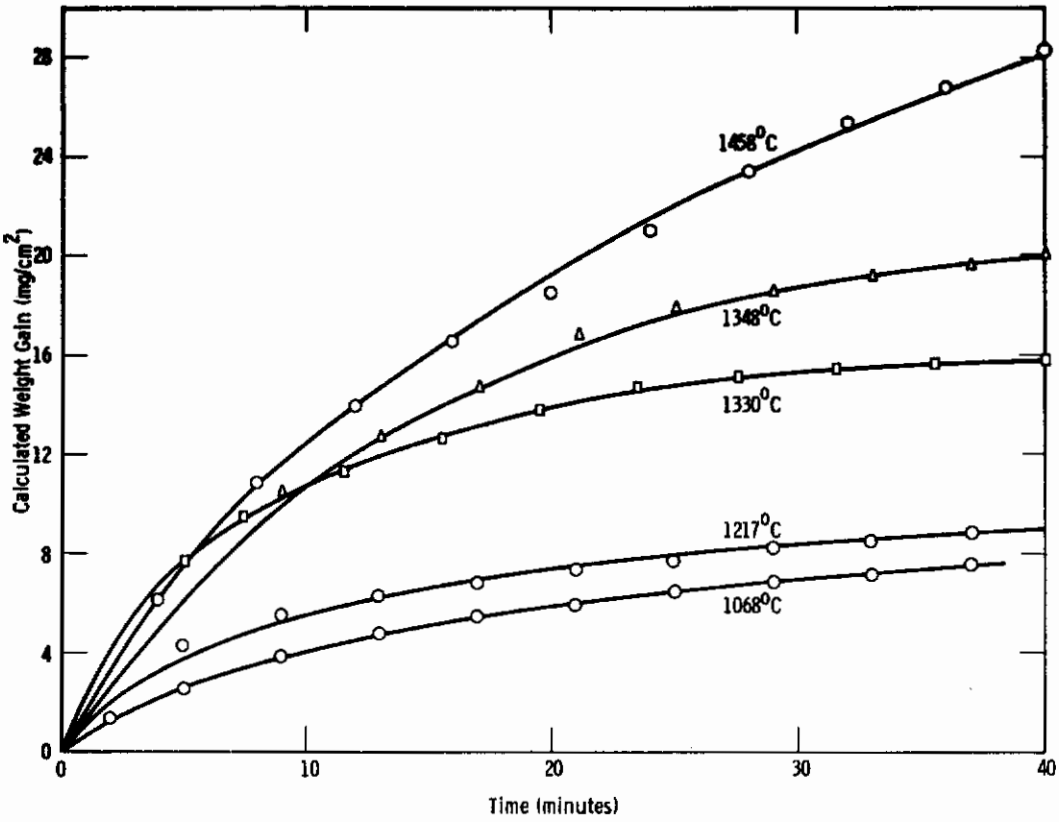

Fig. 23-Oxidation of 50W - 50Ta in 21% O_2 - 79% A heated by radiation

In only one of the experiments, at 1458°C, was there a significant difference between the oxygen consumption computed from the oxygen gauge e.m.f. and the flow rate, and the weight gain of the sample determined from weighings before and after the oxidation. This experiment gave an evaporation rate of WO_3 of 7.1×10^{-6} g/cm^2/sec. This may be compared to the rate of WO_3 vaporization from an oxidizing tungsten sample of 3.0×10^{-4} g/cm^2/sec. The latter value was calculated from measurements given in WADC Technical Report 59-575 Part II. The evaporation rate of WO_3 over the oxide scale formed on the 50 W - 50 Ta alloy is 2.4% of the evaporation rate of WO_3 formed on tungsten. This diminished vaporation rate during oxidation is in excellent agreement with the WO_3 vaporization from $Ta_{10}W_8O_{49}$, which is 2.5% of the WO_3 rate from tungstic oxide.

DISCUSSION

It would appear that the protective oxide scale on 50 W - 50 Ta is the oxide $Ta_{10}W_8O_{49}$. In the oxidation of tungsten at high temperatures reported in WADC Report 59-575 Part II, a very thin tightly adherent blue oxide film was found between the metal and WO_3. This film was thought to be $W_{18}O_{49}$ based on its color. Webb, Norton and Wagner[11]; Speiser[12]; and Gulbransen and Wysong[13] have observed that tungsten forms a protective film at lower temperatures. Webb et al found a thin blue oxide which was not uniquely identifiable from x-ray patterns, but corresponded in some respects to the ASTM x-ray cards for W_4O_{11} (now generally accepted as $W_{18}O_{49}$). Speiser also found the blue oxide which he states is either $W_{18}O_{49}$ or $W_{20}O_{58}$. Both of the latter authors think that the blue oxide is protective.

Since the blue oxide film formed on tungsten appears to grow by diffusion and is thought to be $W_{18}O_{49}$, the protective oxide formed on the 50 W - 50 Ta alloy, $Ta_{10}W_8O_{49}$, is analogous to $W_{18}O_{49}$ with the same metal to oxygen ratio and with a similar WO_3 evaporation rate. By implication it ought to have other properties in common with $W_{18}O_{49}$ which lead to the formation of a protective scale. Among these properties is the tight adhesion of the scale to the underlying metal. Both the blue scale on tungsten and the scale on the 50-50 alloy were extremely difficult to remove.

The volatility of the oxide formed on the 50-50 alloy was small enough to eliminate the necessity for correcting the balance data previously measured up to 1200°C in 0.1 atm of oxygen. These earlier data were used in Figure 24 along with present data for an Arrhenius plot of the parabolic constant. Although there was a considerable deviation from the parabolic shape for many of the curves, it was useful to present the data in this manner for purposes of comparison and extrapolation. The oxygen pressure sensitivity appears to be small compared to scatter of the data so that no correction was made for the pressure differential.

In contrast to both the tungsten rich alloys studied here earlier[8] and the tantalum rich alloys studied by Schmidt et al[8], the 50 W - 50 Ta alloys exhibit protective oxidation behavior at the highest temperature studied, 1458°C. After one hour at 1400°C, this alloy gains only 3 to 4% of the oxygen gained by tantalum and the 5, 10 and 20% W-Ta alloys. After one hour the oxygen weight gain of this alloy at 1200°C was 1.5 to 15% of that gained by tungsten and the 10 and 25% Ta-W alloys. Thus the 50-50 alloy has considerably

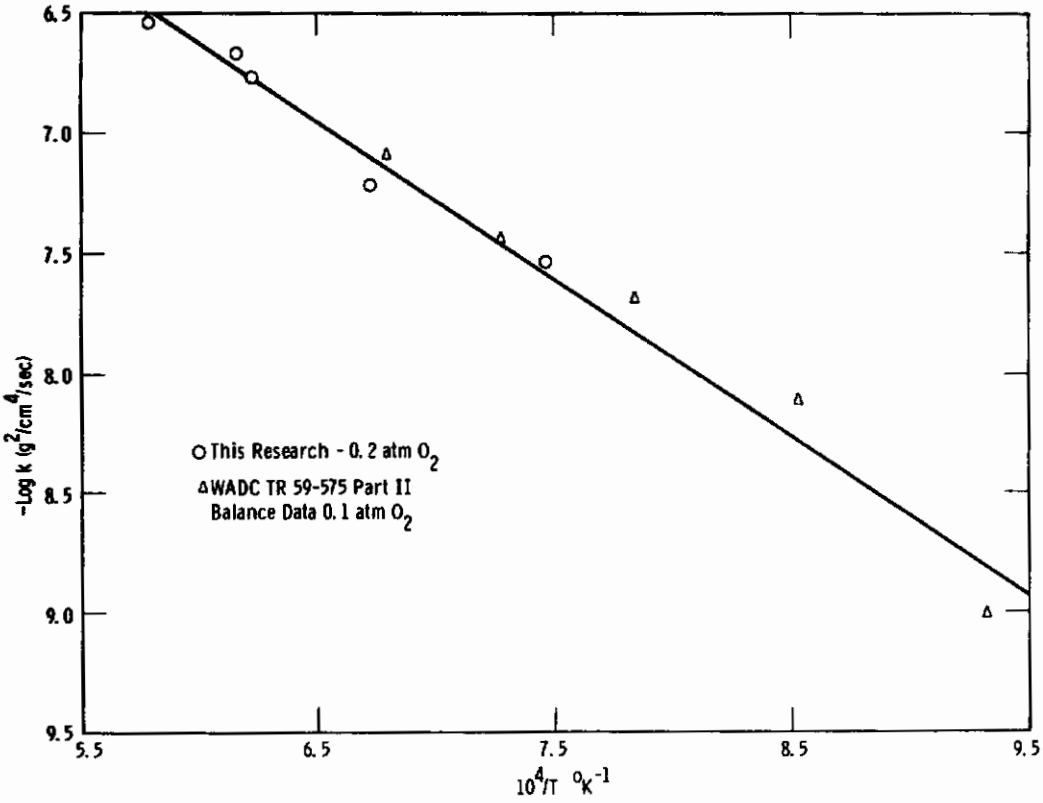

Fig. 24—Log parabolic constant for 50W - 50Ta oxidation vs 1/T

better oxidation resistance than either of the pure metals and it was a significant improvement over other tantalum-tungsten alloys tested.

FUTURE WORK

The experimental results of the study of the oxidation rate of the alloy, 50 W - 50 Ta, show the alloy possesses a high degree of oxidation resistance. Further investigations of its oxidation properties to our limit of 1615°C would prove useful.

With the application of electron diffraction techniques, a study could also be made of the nature of the oxide film formed at various temperatures.

SECTION III. HIGH VOLTAGE ELECTRON DIFFRACTION

INTRODUCTION

Early studies by Langmuir[1] as well as recent studies included in Section I of this work suggests that the rate of reaction was determined by the nature of the reacting interface. It would appear that studies should be undertaken to determine the structure of the interface during oxidation and vaporization of tungsten trioxide. Electron diffraction offers one method for direct study of the interface. Several difficulties occur in studies of this type. First, furnaces must be built to heat tungsten and carry out oxidation reactions "in situ" at high temperatures. Second, high voltage diffraction at electron accelerating voltages well above 100 kv should be used. Third, correlation of the diffraction patterns to known structures have been difficult.

Commercial electron microscopes and electron diffraction cameras operate with accelerating voltages of 30-100 kv. A number of higher voltage instruments were built during the period of 1941 to 1952. The advantages of high voltage electron diffraction were discussed by Finch, Lewis and Webb[14] in 1953. These advantages were confirmed by workers[15,16] in Japan and two instruments were built for 300 kv electrons. A recent publication[17] has shown that the Russians have been using 400 kv electron diffraction cameras since 1957.

The advantages of increasing beam potential above 100 kv are: (1) greater transmission of electrons through thick specimens, (2) a smaller adsorption of energy from the beam, (3) a larger ratio of elastically to inelastically scattered electrons with a corresponding increase in pattern clarity and freedom from background, (4) in reflection from poorly conducting surfaces, smaller disturbances occur due to charging up of the specimen with a corresponding decrease in grazing angle of the beam to the surface and a decrease in depth of penetration from 5 to 6 to 1 to 2 atom layers for flat specimens.

This work will give a brief description of a 250 kv electron diffraction camera for the study of surface reactions at high temperatures. In deciding on building a 250 kv electron diffraction camera, the following technical problems were considered: (1) cost of high voltage supply, (2) space available, (3) adapting to present electron diffraction column and (4) x-ray shielding. Increasing the voltage from 50 to 250 kv was achieved without an increase in space and without a large capital investment. However, certain problems still have to be solved before the operation at the highest voltages can be achieved.

EXPERIMENTAL

The instrument was designed for use at voltages up to 250 kv. Many parts of the column of an older 50 kv electron diffraction camera were used in the new instrument. The major problem was the design of a compact 3 stage electron gun for 250 kv electrons. A new 300 kv D.C. voltage source and a number of D.C. power sources were purchased. The D.C. power sources were used for the electron lenses, electromagnetic tilt coils and deflecting plates.

To minimize contamination which is always a difficult problem in the study of surface reactions a new vacuum and pumping system was developed. A new furnace design for heating specimens to 1100°C was also developed. Since the instrument was designed primarily for high temperature surface reactions, special gas purification trains were built for preparing dry oxygen and dry hydrogen.

Figures 25, 26 and 27 show schematic drawings with the appropriate captions for the several sections of the instrument. Figure 25 shows the gun and voltage divider section for energizing the several stages of the electron gun. Figure 26 shows the main column and Figure 27 shows the furnace unit, specimen chamber and photographic section of the camera.

PRELIMINARY RESULTS

Since the instrument was only recently completed the results presented below are of a preliminary nature.

1. Electron Gun

Electrical problems were found in operating the electron gun above 180 kv. External corona occurred from the corona rings. This problem was readily solved by enclosing the electron gun and voltage divider in a dry box. Internal electrical discharges occurred between the several stages in the gun for voltages above 220 kv. Guard rings and ears were made to minimize the development of high fields within the gun.

2. Furnace

The furnace for heating specimens has been operated at temperatures up to 1100°C. Since the control thermocouple is located on a dummy specimen and the heater element is inside of the block, fluctuations occurred in the specimen temperature. This difficulty is now being corrected.

Since it is highly desirable to study the oxidation and vaporization reactions at temperatures above 1100°C a new type of furnace must be developed using platinum and ceramic parts or by direct electrical heating of strip specimens of tungsten.

3. Calibrating Standards

ZnO smoke and an evaporated film of TlCl were tested as calibration materials. Both were found to be excellent materials for standards. TlCl must be used with care since the material was hydroscopic. For most precise work the comparison standard diffraction pattern should be taken at the same time as the unknown diffraction pattern. This is not possible when studying reactions at high temperatures.

To calibrate the instrument we determine the product of the diffraction ring diameter and the lattice spacing of the particular reflection. This constant is calculated for each reflection and an average value determined.

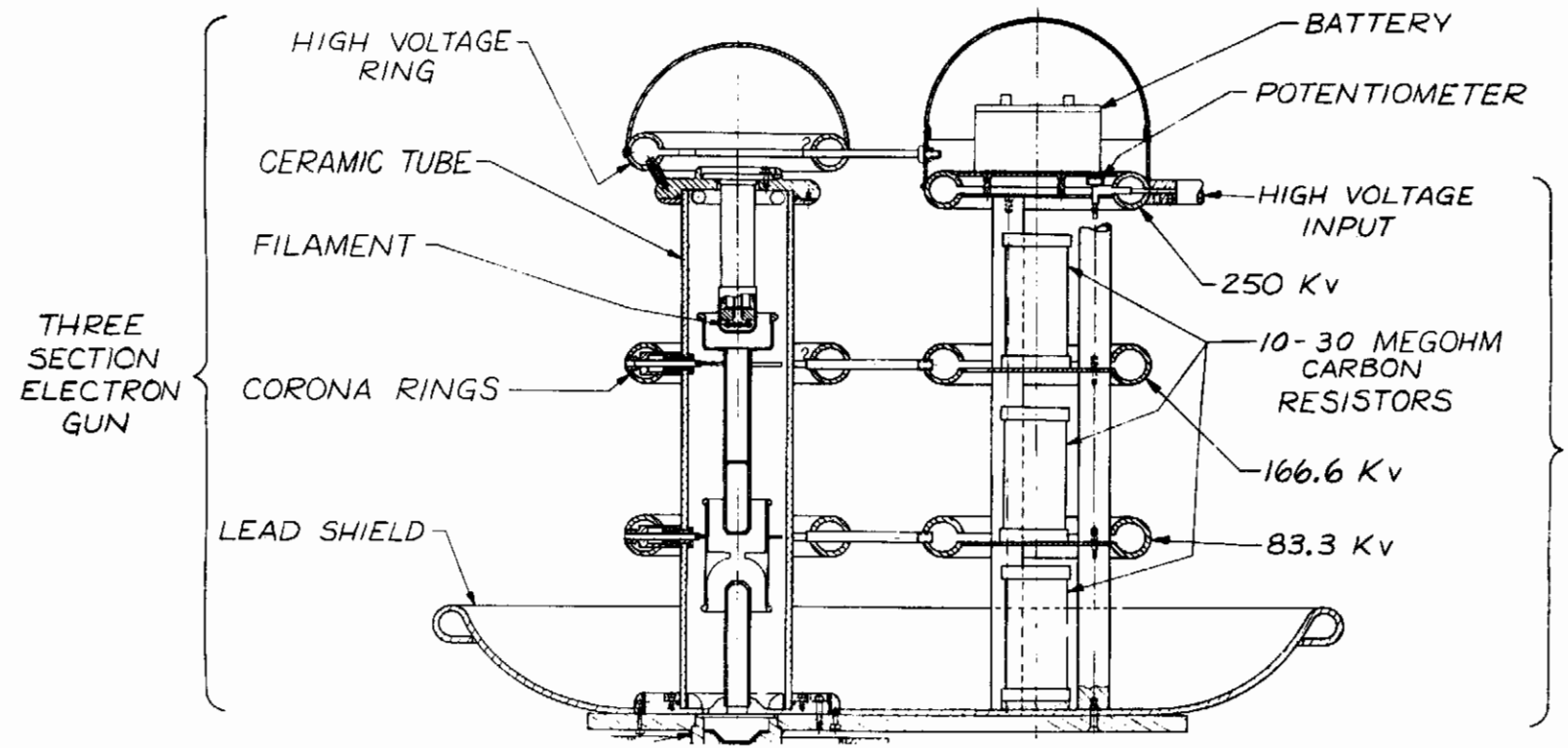

Fig. 25 Electron diffraction-gun and voltage divider

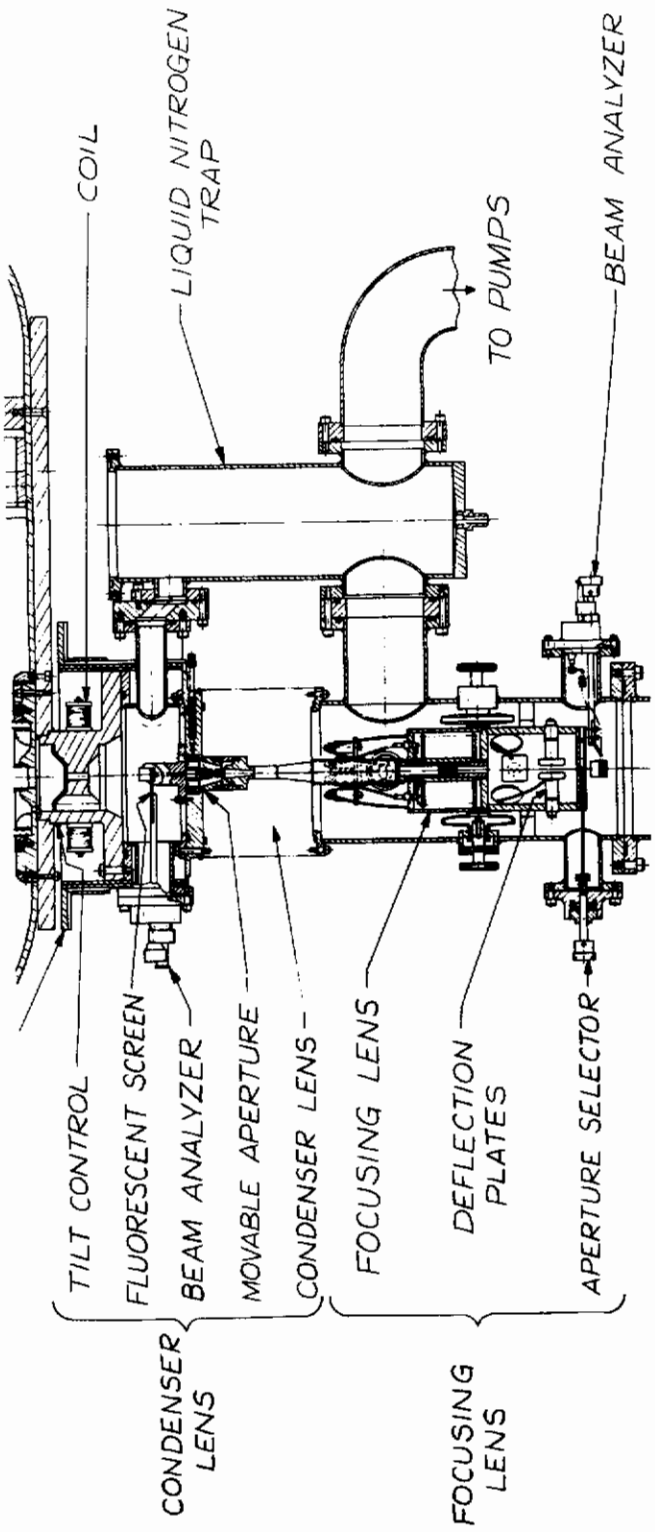

Fig. 26 – Electron diffraction – main column

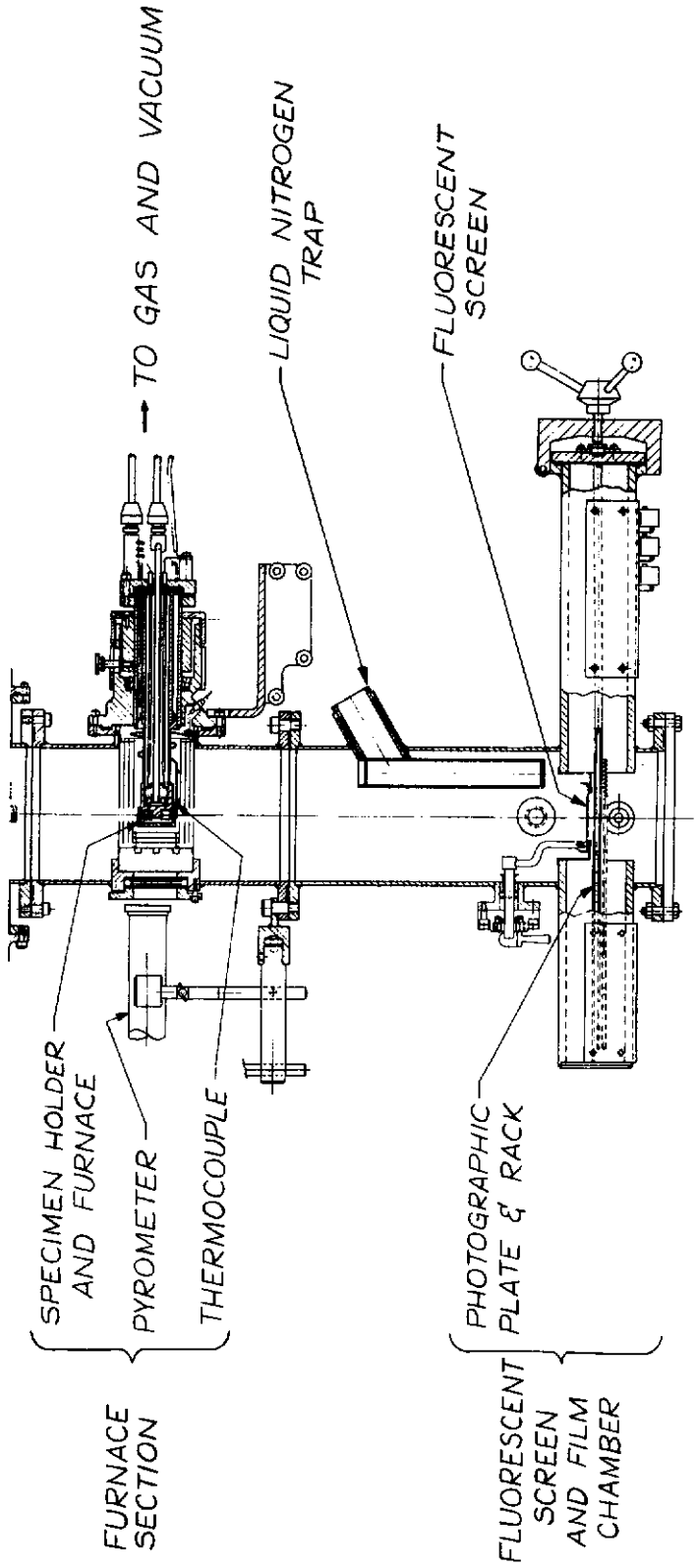

Fig. 27 – Electron diffraction–furnace, specimen chamber and camera

4. Oxidation Studies

Samples of pure tungsten were oxidized at 800°, 900° and 1000°C for 30 minutes "in situ" and diffraction patterns taken at several stages of the oxidation and during evaporation of the oxide using 180 kv electrons. Good electron diffraction patterns were observed. However, the diffraction patterns were not easy to interpret. Further work must be done before the results can be correctly analyzed and discussed.

SECTION IV. THEORETICAL ANALYSES

1. Langmuir's Treatment

Langmuir[1] has treated the reaction kinetics of the clean up of oxygen by a hot tungsten filament. The pressures used were in the range of 10^{-3} to 10^{-2} Torr of oxygen while temperatures were varied from 1070° to 2770°K. The following facts and assumptions were considered in developing a theory to explain the data. (1) Based on electron emission experiments the tungsten surface was considered to be covered with an adsorbed monolayer of oxygen. (2) The condition of the surface responsible for determining the reaction velocity was independent of pressure. This requirement was met by assuming the adsorbed layer was nearly complete and consisted of two kinds of reaction products, WO_2 and WO in equilibrium with each other. Only one type of reaction product, WO, was capable of reacting directly with the oxygen molecules striking the surface. (3) Knudsen's equation was used to calculate the rate of collision of oxygen molecules directly with the surface. (4) The fraction of oxygen molecules striking the surface which react was given by the coefficient ϵ. (5) the following expression was derived for the rate R at which WO_3 was formed from oxygen striking the surface.

$$R = \frac{3\alpha\epsilon_2 P}{\epsilon_2 + 2\alpha(K+1)}$$

Here α was the fraction of all molecules striking the surface which were adsorbed. ϵ_2 was the fraction of oxygen molecules striking a WO molecule which reacts to form WO_3. P was the pressure. K was the equilibrium constant for the equilibrium between fraction of the surface covered by WO_2 and WO. The large temperature coefficient was due to K since ϵ_2 and α were nearly independent of temperature. At low temperatures K was large and R was small. At high temperatures K decreased making R large.

This theory explains qualitatively the behavior of ϵ as a function of temperature since $R = \epsilon p$.

2. Absolute Reaction Rate Theory

This theory when applied to a surface reaction assumes the formation of a complex between the reacting gas and the surface, the surface oxygen layer and the reacting gas, the chemisorbed gas and the surface oxygen layer, and the chemisorbed reaction product and the surface. This development includes some of the features of Langmuir's treatment. In addition, the absolute reaction rate theory could be used to treat the complex reaction as a series of successive steps. The rate of any one of these surface reactions may be considered in terms of reaction complexes passing from one region of configuration space to another[5, 18, 19]. Along a given reaction path there exists one region of configuration space separating the initial and final states having a maximum free energy. According to Eyring and coworkers[19], the number of reaction complexes passing through this region is given by

$$\frac{-dc}{dt} = \sum_{n,i} H_{n,i} C_{n,i} \nu_{n,i}$$

where C = total number of complexes in initial state at time t
H = probability that the reaction complex crosses the barrier in any one attempt
ν = frequency with which the complexes cross the energy barrier
n,i = quantum numbers associated, respectively, with the degree of freedom along the reaction coordinate and with the remaining degrees of freedom of the reaction complex

To carry the theory along further, two approaches have been used. The first utilizes a quantum-mechanical method for calculating the energy of activation. This is difficult, even if approximation methods are used and good agreement is not achieved. The second approach utilizes the experimental activation energies together with an evaluation of the partition functions of the initial and activates states. From this method it has been possible to calculate absolute rates for surface reactions which are in agreement with the experimental ones. The transmission coefficient, H, has been considered in some detail by Hirschfelder [20,21] and Wigner[20], who state that only in exceptional cases does H differ from unity.

In correlating the predictions of the absolute reaction rate theory with experiment, the method of experimental activation energies is used plus partition functions for evaluating the equilibrium between initial and activated states. This method is applied to the various surface processes of adsorption, chemical reaction, and desorption. An analysis of the predicted rate of reaction with experiment is used to suggest a possible mechanism for the oxidation reaction.

Figure 28 shows a coordinate diagram of energy vs. reaction distance for three processes of chemi-sorption, chemical reaction, and desorption. The values of ϵ_1, ϵ_2, ϵ_3 represent the energies of activation of forming the activated complex which exists at the maximum of the energy curves. The dashed line at the center represents the tungsten-O layer about which adsorption and desorption takes place. Two oxygen atoms must be adsorbed about a tungsten-oxygen ensemble for reaction to occur. Because this tungsten-oxygen combination was involved in the tungsten trioxide that was formed, the reaction coordinate was not shown here for the chemical reaction process.

Three schematic equations are given in Figure 28. The chemisorbed bonds are denoted by the dashed line and indicate distances greater than the normal W-O or W-W bond.

Let us now describe the rate equations as given by the absolute reaction rate theory.

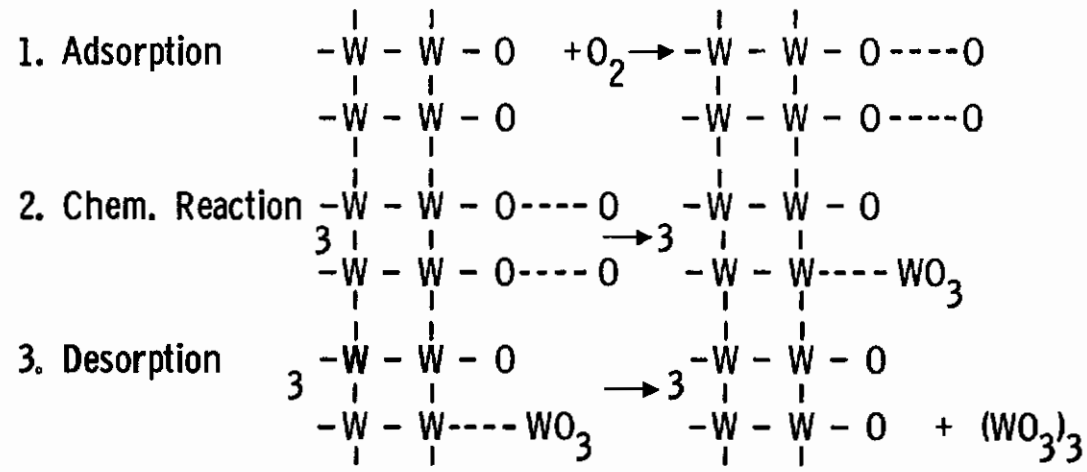

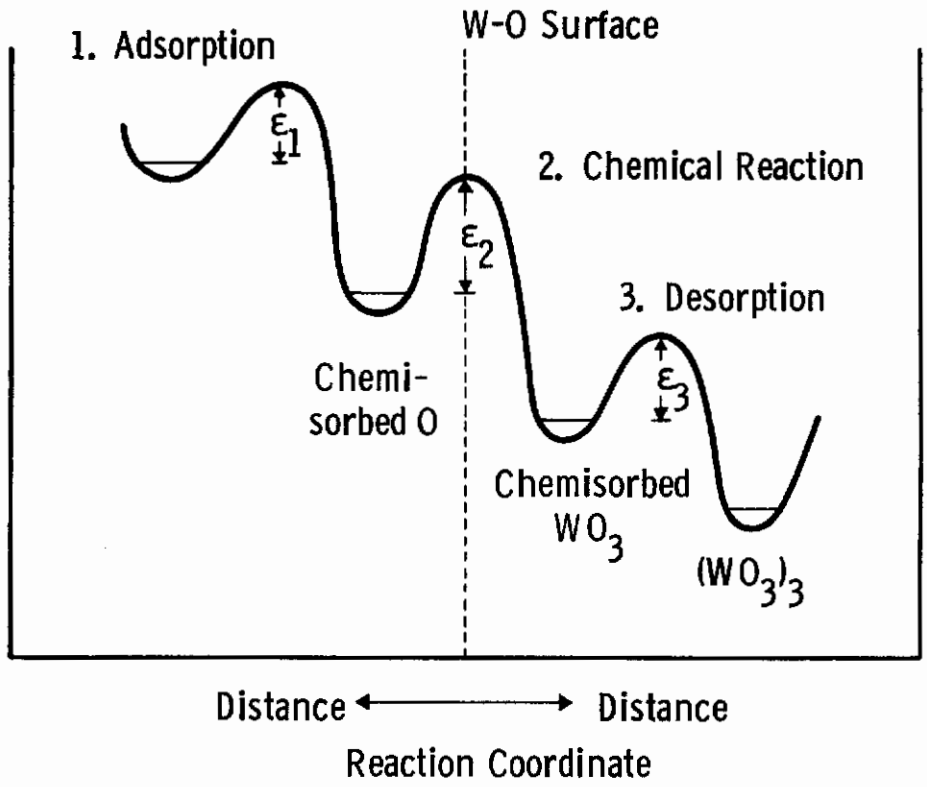

Fig. 28—Energy vs. reaction coordinate curves for processes involved in oxidation of tungsten.

(a) Rate of Adsorption

Adsorption processes [5, 19] may be considered as bimolecular reactions involving an atom or a molecule from the gas phase and an active point in a fixed position on the adsorbing surface. An activated complex is assumed to form between the molecule or atom and the fixed point on the surface. The rate of adsorption is given by the rate of passage of this complex over the potential energy barrier. According to postulates of the theory[14,21], equilibrium exists between molecules of the gas, adsorption centers, and activated complexes. For ideally behaving compounds

$$K = \frac{C^{\ddagger}}{C_g C_s} = \frac{f^{\ddagger'}}{(f_g/V) f_s}$$

where the f terms are complete partition functions of the indicated species. Let $F_g = f_g/V$ or partition function for unit volume of gas; then

$$\frac{C^{\ddagger}}{C_g C_s} = \frac{f^{\ddagger'}}{F_g f_s}$$

According to the theory, the rate of adsorption of gas on the sites of the (i)th kind per square centimeter is given by

$$v_{1(i)} = C_g C_{s(i)} \frac{kT}{h} \times \frac{f^{\ddagger}}{F_g f_s}$$

$f^{\ddagger}$ differs from $f^{\ddagger'}$ by the removal of one degree of translational freedom in the reaction coordinate.

Extracting the zero-point energy contribution

$$v_1 = C_g C_s \frac{kT}{h} \times \frac{f^{\ddagger}}{F_g f_s} e^{-\epsilon_1/kT}$$

To apply the above relationship, several types of adsorption processes may occur, depending upon whether the atom or molecule forms a mobile or immobile layer and whether the adsorption process or the dissociation process is rate-determining. The partition functions for the various degrees freedom are substituted directly in the equation.

Eyring and coworkers [4, 19] have given the following expressions for the several types of adsorption processes.

(1) Immobile Adsorption, Adsorption of Molecule, Rate-Determining

$$v_1 = C_g C_s \frac{\sigma}{\sigma^{\ddagger}} \frac{h^4}{8\pi^2 I (2\pi mkT)^{3/2}} e^{-\epsilon_1/kT}$$

(2) Immobile Adsorption, Dissociation Is Rate-Controlling Process

$$v_1 = C_g^{1/2} C_s \, kT \frac{h^{3/2}}{(2\pi mkT)^{3/4} (8\pi^2 IkT)^{1/2}} e^{-\epsilon_1/kT}$$

(3) Mobile Adsorption

$$v_1 = C_g \frac{kT}{h} \frac{h}{(2\pi mkT)^{1/2}} e^{-\epsilon_1/kT}$$

(4) Mobile Adsorption, No Activation Energy

$$v_1 = \frac{p}{(2\pi mkT)^{1/2}}$$

Here the symbols have the following definitions:

C_g = concentration of molecules per cubic centimeter in the gas phase,
C_s = concentration of adsorption sites per square centimeter,
σ = symmetry number of the gas molecule,
$\sigma^{\ddagger}$ = symmetry number of the activated complex,
h = Planck's constant,
I = moment of inertia,
k = Boltzman's constant,
m = mass of molecule,
T = absolute temperature, and
ϵ = energy of activation.

(b) Rate of Desorption

Desorption from an immobile layer may be regarded as involving an activated state in which a molecule attached to an adsorbing center acquires the necessary configuration and activation energy to permit it to escape from the surface. In the following rate expressions given by Eyring and coworkers [5,19] both activated complexes and adsorbed molecules are considered immobile.

$$v_2 = C_a \frac{kT}{h} e^{-\epsilon_2/kT}$$

Here v_2 represents the rate of desorption in molecules per square centimeter per second, C_a represents the concentration of adsorbed molecules per square centimeter, and ϵ_2 is the energy of activation.

(c) Chemical Reaction

Let us assume the reaction involves one molecule of oxygen and the active surface site, S. This active site is assumed to consist of a site on which oxygen has been previously adsorbed. The activated complex consists of an adsorbed molecule which has acquired the appropriate amount of energy and the proper configuration.

(1) First-Order Kinetics

Consider the case when the active sites already have an oxygen atom attached to the tungsten atoms. If the surface is covered with W atoms having one oxygen atom adsorbed per tungsten atom, the concentration of sites C_s is nearly constant and identical with the number of sites for a bare surface. Under these conditions the rate of the reaction is proportional to the concentration of the molecules in the gas phase C_g and the reaction is of first order.

The rate expression is

$$v = C_g C_s \frac{\sigma}{\sigma^\ddagger} \times \frac{1/2 \; sh^4}{8\pi^2 I(2\pi mkT)^{3/2}} e^{-\epsilon_3/kT}$$

where s is the total number of possible sites adjacent to any reaction center, σ and $\sigma^\ddagger$ are the symmetry numbers of the molecules of reactant and activated complex, respectively, and ϵ_3 is the energy of activation for this type of reaction.

(2) Zero-Order Kinetics

Let us assume the active site already has an oxygen atom attached and that these sites are covered by adsorbed molecules to an appreciable extent. The value of C_s varies with the pressure of the gas. If the surface is nearly covered by adsorbed molecules, C_s is nearly constant and the rate of reaction is nearly independent of the pressure. The following equation treats the reaction from the viewpoint of the adsorbed molecules, with the surface activation energy being the difference in energy between the activated state and the adsorbed reactants, or $\epsilon_0 + \epsilon$:

$$v_2 = C_a \frac{kT}{h} e^{-E/RT}$$

where E is the observed activation energy, ϵ is the heat of adsorption, and ϵ_0 is the difference in energy between the activated state and the initial gaseous reactant.

3. Comparison of Theory with Experiment

Table 5 shows a comparison of the rates of the various processes at 1465°C and 19 Torr oxygen pressure as predicted from the absolute reaction rate theory with the experimentally determined rate of reaction. The calculations were based on an experimental heat of activation of 14,300 calories per mole. The fact that several processes occur with a theoretical rate slower than the experimental value means the heat of activation was too high for this particular process. The comparison was significant only for those processes which give reasonable agreement.

The only feasible mechanism according to Table 5 is mobile adsorption of oxygen molecules on a tungsten surface already covered with an surface layer of oxygen. Even here the agreement between theory and experiment was not good. The effect of pressure on the rate of oxidation was in agreement with the rate expression.

TABLE 5

Correlation of Predictions of Absolute Reaction Rate Theory With Experimental Rate of Oxidation of W at 1465°C and 19 Torr

Mechanism	Equation	Rate (No. W atoms/cm^2/sec) Theory	Experiment
Immobile adsorption, adsorption of molecule, rate-controlling	$v_1 = C_g C_s \frac{\sigma}{\sigma^\ddagger} \frac{h^4}{8\pi^2 I(2\pi mkT)^{3/2}} e^{-\epsilon_1/kT}$	4.2×10^{13}	2.6×10^{18}
Immobile adsorption, dissociation rate-controlling	$v_1 = C_g^{1/2} C_s \frac{kT}{} \frac{h^{3/2}}{(2\pi mkT)^{3/4}(8\pi^2 IkT)^{1/2}} e^{-\epsilon_1/kT}$	1.8×10^{22}	2.6×10^{18}
Mobile adsorption, no activation energy (Hertz-Knudsen equation)	$v_1 = \frac{p}{(2\pi mkT)^{1/2}}$	2.8×10^{21}	2.6×10^{18}
Mobile adsorption	$v_1 = C_g \frac{kT}{h} \frac{1}{(2\pi mkT)^{1/2}} e^{-\epsilon_1/kT}$	4.5×10^{19}	2.6×10^{18}
Desorption	$v_3 = C_a \frac{kT}{h} e^{-\epsilon_3/kT}$	8.1×10^{26}	2.6×10^{18}
Chemical reaction, first-order kinetics	$v_2 = C_g C_s \frac{\sigma}{\sigma^\ddagger} \frac{1/2\ sh^4}{8\pi^2 I(2\pi mkT)^{3/2}} e^{-\epsilon_2/kT}$	8.4×10^{13}	2.6×10^{18}
Chemical reaction, zero-order kinetics	$v_2 = C_a \frac{kT}{h} e^{-\epsilon_2/kT}$	8.1×10^{26}	2.6×10^{18}

SECTION V. SUMMARY AND CONCLUSIONS

In this report we have presented results on the following problems: (1) the kinetics of oxidation of tungsten over the temperature range of 1150° to 1615°C and for pressures from 2 to 100 Torr of oxygen, (2) the kinetics of oxidation of a 50 w/o Ta - W alloy at 152 Torr oxygen pressure and for the temperature range of 1068° to 1468°C. Several pieces of experimental apparatus were built or refined to aid in the studies. These include: (1) a Kanthal-Super furnace to heat the alumina furnace tubes to 1600°C, (2) an oxygen consumption apparatus for measuring fast oxidation reactions and (3) a 250 kv electron diffraction camera for surface interface studies at high temperatures.

The reactions of tungsten with oxygen as a function of temperature and pressure vary greatly. Four types of behavior were noted: (1) formation of a protective oxide film, (2) formation of a non-protective oxide scale, (3) simultaneous formation of an oxide scale and vaporization of tungsten trioxide, and (4) formation of tungsten trioxide gas without formation of an appreciable oxide film or scale.

Types 3 and 4 oxidation curves were studied in detail by both the weight change method and oxygen consumption measurements. Both measurements are required for type 3 oxidation curves to determine the course of the reaction. Above 1250°C all of the oxidation rate curves followed type 4 behavior. Experiments on type 4 oxidation curves showed that surface recession values could be obtained directly from weight change measurements or by calculation from oxygen consumption measurements.

The effect of temperature on the oxidation of tungsten was studied for four pressures over the temperature range of 1250° to 1615°C. The initial rate of weight loss values followed an exponential function of temperature. A heat of activation of 14,300 calories per mole was estimated.

A study of the effect of pressure also was made. The following rate law was found to fit the data, $K = ap^{1.122}$.

The following empirical rate law equation was determined for the data

$$\frac{dw}{dt} = 1.87 \times 10^{-3} \; p^{1.122} \; e^{-14{,}300/RT}$$

An analysis was made of the heat effects associated with the high rates of oxidation. For the oxidation at 1465°C and 49 Torr oxygen pressure the experimental value for the tungsten weight loss was 4.22×10^{-3} g/cm^2/sec. The heat rate for this rate of reaction was 2.4 cals/sec. Assuming the heat was removed by radiation, a temperature rise of 113°C must result if the tungsten surface was assumed to have an emissivity of 1. The high heat rates associated with the rapid oxidation reaction may account for the scattering in the experimental results.

Studies were made on the oxidation of a 50 weight percent tungsten-tantalum alloy over the temperature range of 1068° to 1458°C at 152 Torr oxygen pressure. The data show that a protective scale is formed on this alloy. The oxidation resistance was considerably improved over the pure metals or of other tungsten-tantalum alloys.

A 250 kv electron diffraction camera with high temperature furnaces was built for study of the tungsten-oxygen reaction interface. Preliminary results are being obtained on the oxidation of tungsten at 800° to 1000°C.

A theoretical analyses was made of the kinetic data. A mechanism of mobile adsorption on to an oxygen covered tungsten surface was found to be rate controlling. However, the agreement between the calculated and experimental rate expressions was not as good as was hoped.

LIST OF REFERENCES

1. I. Langmuir, "Chemical Reactions at Very low Pressures, I. The Clean-up of Oxygen in a Tungsten Lamp," J. Am. Chem. Soc., 35, 105 (1913) and "Chemical Reactions at Low Pressures," ibid. 37, 1139 (1915).

2. R. A. Perkins and D. D. Crooks, "Low-Pressure, High Temperature Oxidation of Tungsten," J. of Metals, 13, 490, (1961).

3. E. A. Gulbransen and K. F. Andrew, "Mullite and Zircon Furnace Tubes for High Temperature and High Vacuum Systems; A New Method for Measuring Pressure," Ind. & Eng. Chem. 4, 2762-7 (1949).

4. S. Glasstone, K. J. Laidler and H. Erying, Theory of Rate Processes, New York, McGraw-Hill Book Co., 1941.

5. O. Kubaschewski and E. Evans, Metallurgical Thermochemistry, Acad. Press (1951).

6. W. H. McAdams, Heat Transmission, McGraw-Hill Book Co., 1954.

7. E. G. King, W. W. Weller, and A. U. Christensen, "Thermodynamics of Some Oxides of Molybdenum and Tungsten," Bureau of Mines Report of Investigations 5664, U. S. Gov't. Printing Office, Washington (1960).

8. F. F. Schmidt, W. D. Klopp, W. M. Albrecht, F. C. Holden, H. R. Ogden, and R. I. Jaffee, "Investigation of the Properties of Tantalum and Its Alloys," WADD TR 59-13, (March 1960).

9. J. Weissbart and R. Ruka, "Oxygen Gauge," Rev. Sci. Instr., 32, 593 (1961).

10. C. Wagner and K. Grünewald, Z. physik. Chem., 40B, 455 (1938).

11. W. W. Webb, J. T. Norton, and C. Wagner, "Oxidation of Tungsten," J. Electrochem. Soc., 103, 107 (1956).

12. R. Speiser, "Research on the Oxidation Behavior of Tungsten," AF 33(616)-5721, Report 831-4, (1959).

13. E. A. Gulbransen and W. S. Wysong, "Thin Oxide Films on Tungsten," Am. Inst. Mining and Met. Eng., Inst. of Metals Div., 175, 611 (1948).

14. G. I. Finch, H. C. Lewis, and D. P. Webb, "Diffraction of 150 KV Electrons," Proc. Phys. Soc. 66B, 949 (1953).

15. H. Watanabe, S. Nagakura, N. Kato, "Application of 300 KV Electron Microscope", Proceedings of the First Regional Conference in Asia and Oceania, Toyko, (1956).

16. B. Tadano, Y. Sakaki, S. Maruse, and N. Morito, "New 300 KV Electron Microscope, "J. Electronmicroscopy, 4, (Annual Edition), (1956).

17. N. M. Popov, "Electron Microscope-Diffraction Camera with a 500 KV Accelerating Potential." Bull. Acad. Sci. U.S.S.R., Phys. Ser. 23, No. 4, April (1959).

18. H. Eyring, C. B. Colburn, and B. J. Zwolinski, "The Activated Complex in Chemisorption and Catalysis," Discussions Faraday Soc. No. 8, 39-46 (1950).

19. K. J. Laidler, S. Glasstone, and H. Eyring, "Application of the Theory of Absolute Reaction Rates to Heterogeneous Processes," J. Chem. Phys. 8, 659-76 (1940).

20. J. O Hirschfelder and E. Wigner, "Some Quantum-Mechanical Considerations in the Theory of Reactions Involving an Activation Energy," J. Chem. Phys. 7, 616, (1939).

21. H. M. Hulburt and J. O. Hirschfelder, "The Transmission Coefficient in the Theory of Absolute Reaction Rates," J. Chem. Phys. 11, 276 (1943).